5.1 Introduction

5.1.1 Cross-coupling reactions

Cross-coupling reactions such as the Heck, Suzuki-Miyaura, Sonogashira, Buchwald-Hartwig are ranked among the most powerful and versatile organic reactions (Scheme **5.1**) [1,2]. The advent of these organic transformations have enabled the development of expedient synthetic routes for the construction of C–C, C–O, C–N functionalities having varied pharmaceutical and industrial applications [3]. Advancement in cross-coupling technology has provided new synthetic routes for drug design over conventional methods. For instance, the preparation of anti-hypertensive drug losartan involves a late-stage Suzuki–Miyaura reaction [4]. Cross coupling reactions represent a comparatively mature technology, whose foundations were laid by the works of renowned scientists Heck, Suzuki and Negishi for which they were awarded the Nobel Prize in Chemistry [2,5]. Generally, cross coupling reactions are those in which two different fragments are joined in the presence of a transition metal catalyst [6]. Although several metal centres are effective of catalyzing various steps of these reactions, but in most cases catalysts based on palladium dominate the scene.

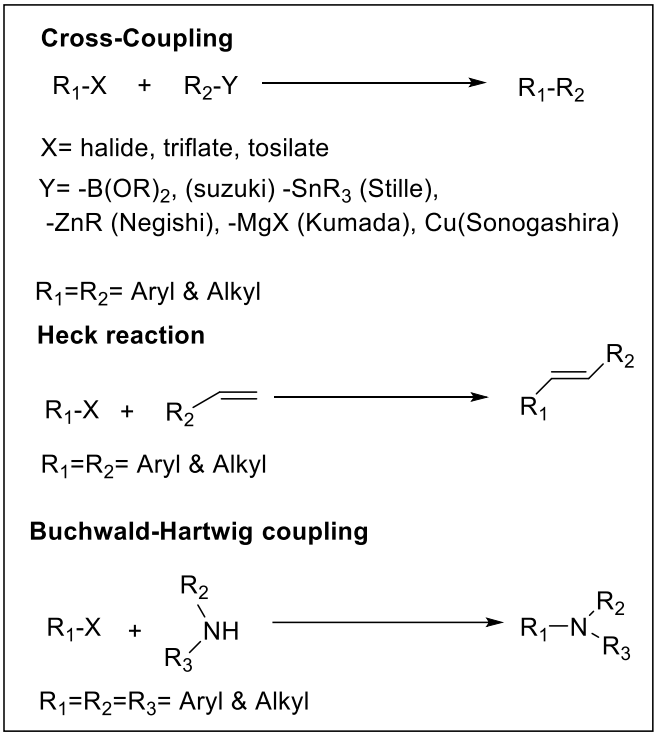

Scheme **5.1** Schematic representation of various cross-coupling reactions

Palladium (Pd) is so far the most popular and promising metal used in cross-coupling reactions [7]. The high versatility, broad substrate scope tolerance, remarkable functional group compatibility and mild reaction conditions of cross-coupling reactions especially with palladium catalysts have not only changed the landscape of organic chemistry, but also have profoundly impacted pharmaceuticals, material science and other related industries [8]. Homogeneous Pd catalyst preformed or generated *in situ* upon addition of ligands such as phosphines, carbenes, amines, are commonly employed for cross-coupling and related reactions [9]. Despite significant growth in attaining higher activity, enhanced selectivity and broader substrate scope; homogeneous Pd catalysis suffer from serious disadvantages such as toxicity, use of expensive ligands, product contamination due to difficulty in separation of the residual metal and reusability of the catalyst [10,11].

In recent times, extensive research has been underway on catalysts based on highly dispersed nanosized Pd metal on a solid support. These materials were found to deliver excellent catalytic performances for cross-coupling reactions and could often be recovered and recycled, which adds to their economical significance [12]. The manufacture and application of heterogeneous catalytic systems based on Pd metal for varied cross-coupling reactions has been continuously under study to produce catalysts with high activity, selectivity, reusability and durability [13].

5.1.2 Suzuki-Miyaura cross-coupling (SMC) reaction

The C–C cross-coupling reaction has become truly fundamental in natural product synthesis, material sciences, medicinal and supramolecular chemistry. Undoubtedly, the most extensively investigated route towards C–C bond formation reaction is the Suzuki–Miyaura cross-coupling reaction that provides rapid access to biaryl motifs *via* sp^2–sp^2 linkages [3,14]. The palladium catalysed coupling of organoboranes with organic halides in presence of a base; termed as the Suzuki–Miyaura coupling (SMC) reaction, one of the most elegant and effective methods for carbon–carbon bond formation (Scheme **5.2**) [15].

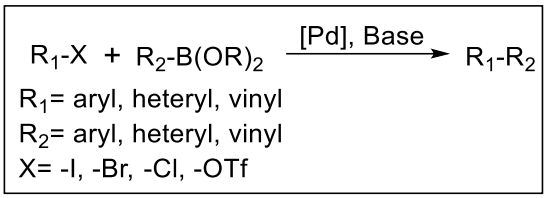

Scheme **5.2** Schematic representation for Suzuki-Miyaura cross-coupling reaction

In particular, the high success rate of SMC reactions is remarkable. A major reason for the widespread use of this cross-coupling reaction is their reliability and reproducibility compared to other synthetic methods [16]. The key advantages of this cross-coupling reaction are the mild reaction conditions, commercial availability of an array of precursors, functional group compatibility, stability towards air and moisture and use of easily synthesizable and nontoxic boronic acids [17]. A recent review by Roughley and Jordan stated that 62% of the total C–C bond forming processes utilised for preparing drugs involved cross-couplings catalysed predominantly by Pd (Figure **5.1**).

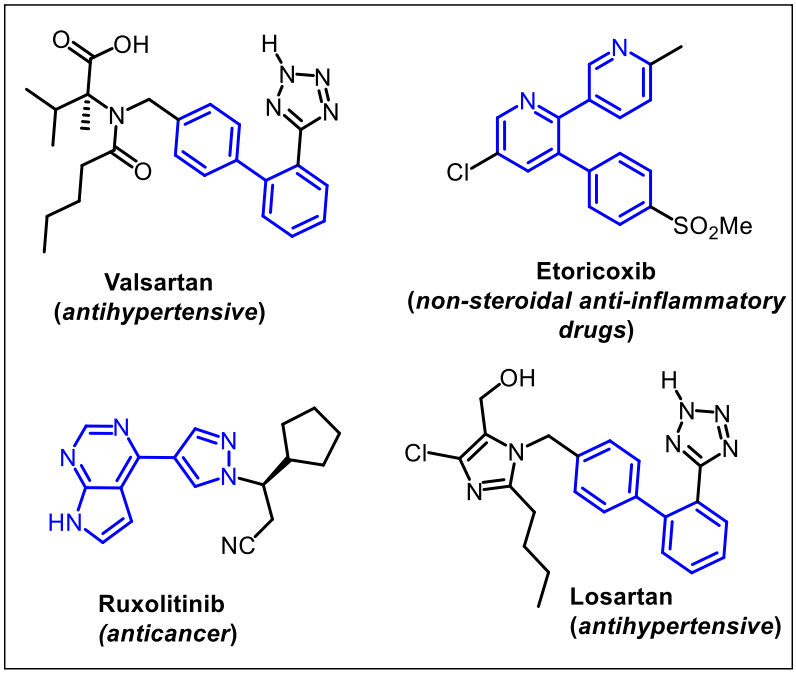

Figure **5.1** Drug molecules containing C-C bond

Even though Pd catalysed cross-coupling is already a matured field, current rate of demand towards heterogeneous Pd catalysts for long-term sustainability due to high cost and low natural abundance of Pd for various transformations is still in demand [18]. One favourable approach for sustainable synthesis is to develop a

reusable catalyst that can be completely removed from the reaction mixture and is recyclable without significant loss of catalytic activity [19].

5.1.3 Denitrative cross-coupling reaction

Nitroarenes are abundant chemical feed stocks and denitrative transformations of nitroarenes are advantageous in synthetic chemistry due to its easy preparation by electrophilic aromatic nitration of arenes from simple starting materials [20,21]. Nitro compounds act as synthetic intermediates allowing access to haloarenes *via* reduction, diazotization and halogenations and also utilized for preparing heterocyclic compounds. The electron-withdrawing nature of the nitro group can function as a transient leaving group to effectively transform into other important functionalities [21-23].

Surprisingly, the use of nitroarenes in cross-coupling has been limited due to lack of a capable metal catalyst to efficiently cleave the C–NO_2 bond. Despite the relative inertness of C–NO_2 bond toward transition metal catalysts, the –NO_2 group itself often causes undesired deactivation of metal catalysts. Due to these drawbacks, the development of denitrative transformations has been regarded as challenging in cross-coupling chemistry. The combination of palladium as a metal centre and BrettPhos as a supporting ligand enabled the unprecedented oxidative addition of Ar–NO_2 bonds to Pd(0) to enable the SMC, Buchwald–Hartwig amination, and ether synthesis. Although these coupling reactions opened a novel aspect in chemistry of nitroarenes, there still remains enormous opportunities to explore in this arena [21].

5.1.4 Denitrative ether synthesis

Ethers are one of the most valuable functional groups representing an important class of intermediates for pharmaceuticals, agrochemicals and polymers. Diphenyl ethers find applications in agrochemical as fungicides and herbicides; while phenolic ethers find applications in chemical engineering, pharmaceuticals and food [24,25]. They are also important precursors for polymers and fragrances. Organic ethers have found significant applications as pharmaceuticals, drug intermediates, disinfectants, herbicides, plasticizers and solvents. Ethers have been synthesized by

different protocols such as Williamson ether synthesis, Ullmann coupling, the Mitsunobu reaction, bimolecular dehydration and transition metal-free coupling reaction (Scheme **5.3**) [26]. Drawbacks encountered in many conventional techniques such as high catalyst loadings, elevated temperatures, catalyst deactivation necessitated the search for an alternative route to enhance conversion rate and reduce environmental pollution. Surprisingly, reactions involving denitration for ether synthesis are still limited in literature and require extensive investigation.

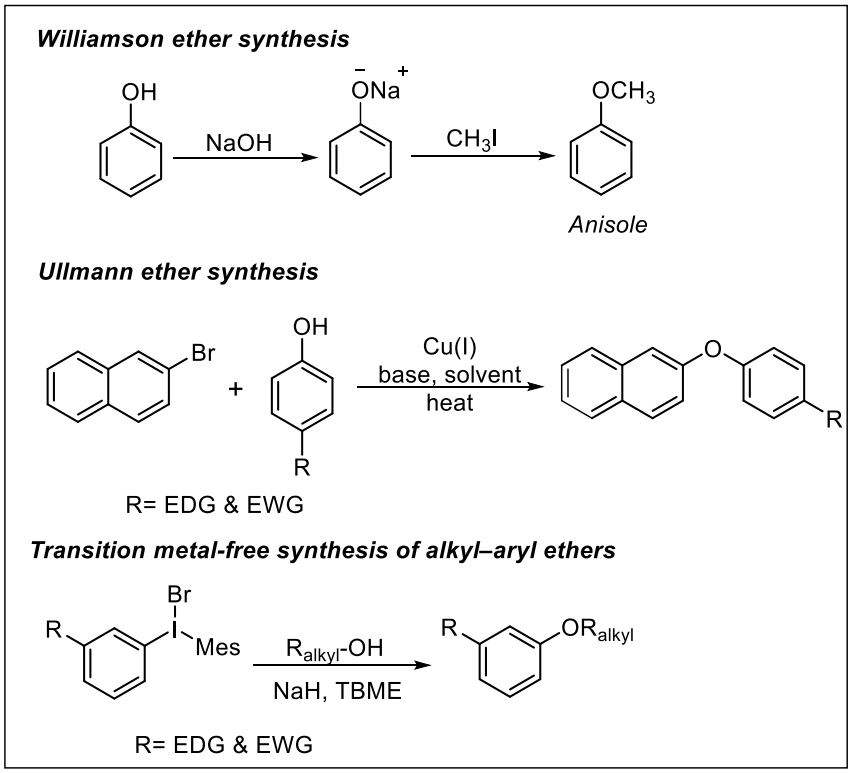

Scheme **5.3** Conventional methods for synthesis of ethers

In 2012, Wu's group reported denitrative diaryl ether synthesis using phenol and $Cu(OAc)_2 \cdot H_2O$ as catalyst, Cs_2CO_3 as base in DMF under N_2 atmosphere (Scheme **5.4**) [27]. Chang group in 2013 reported first Pd catalysed protocol for the denitrated coupling reaction of nitroarenes with phenols. The prepared cyclopalladated ferrocenylimine complex exhibited high catalytic activity for this transformation with low catalyst loading and shorter reaction time (Scheme **5.4**) [28]. Bora et al., in 2017 established a denitrative diaryl ether synthesis using Pd/C as a heterogeneous catalyst and also carried out mechanistic study. Electron-

deficient nitroarenes coupled with phenols in presence of Pd/C, K_2CO_3, and H_2O in DMSO, afforded the corresponding diaryl ethers in good yields (Scheme **5.4**) [29]. In 2019, the Ghaderi group reported nickel-catalysed denitrative etherification. $NiCl_2$ and K_3PO_4 in molten tetrabutylammonium bromide (TBAB) at 100 °C allowed denitrative coupling between nitroarenes and alcohols to give ether. Both phenols and primary alcohols took part in this reaction (Scheme **5.4**) [30].

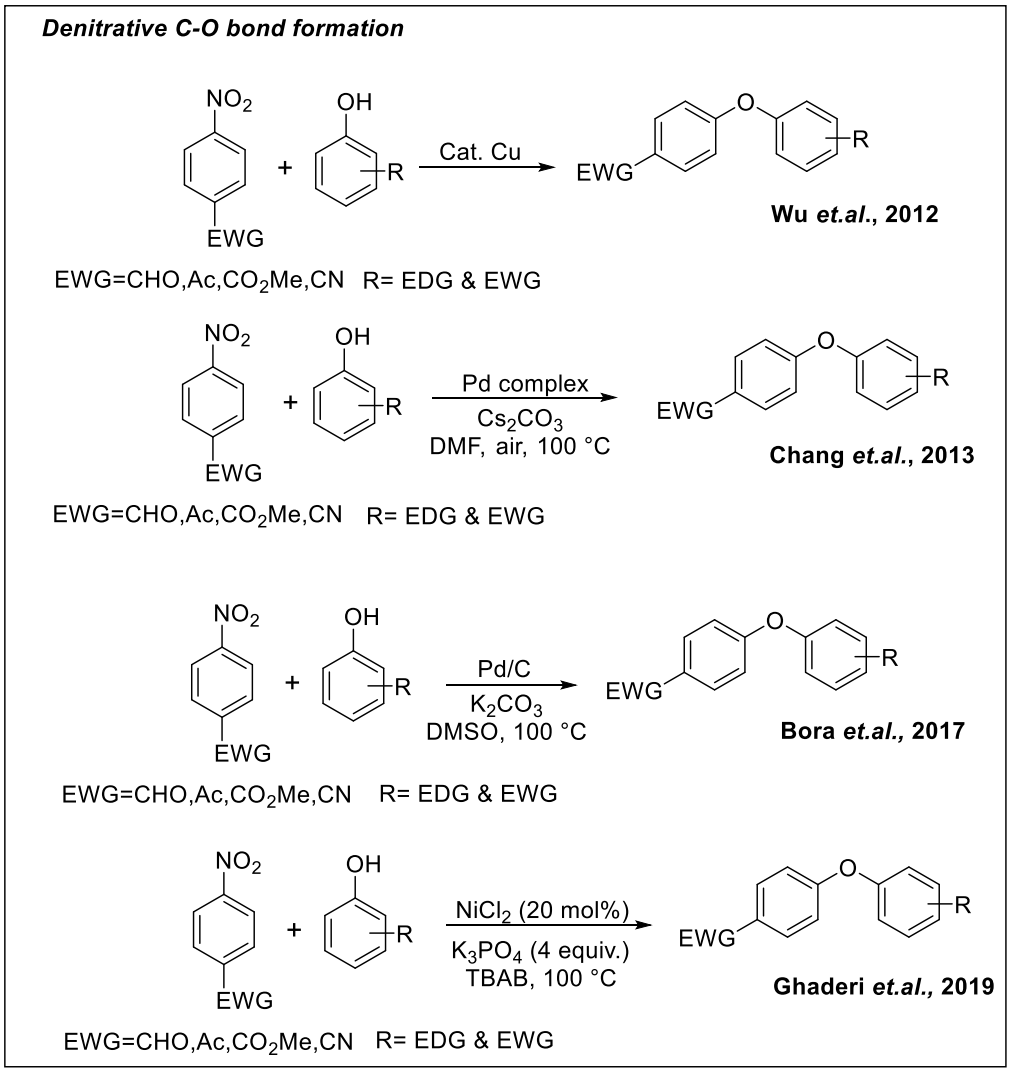

Scheme **5.4** Denitrative ether synthesis

5.1.5 Other Denitrative cross-coupling reactions

5.1.5.1 Denitrative Suzuki–Miyaura coupling

Denitrative reactions have promoted the utility of nitroarenes as aryl sources in coupling reactions. A pioneering report appeared in 2017 by the group of Nakao where a general denitrative Suzuki–Miyaura-type coupling was developed by using

palladium as catalyst. Extensive screening revealed that the use of $Pd(acac)_2$, BrettPhos, $K_3PO_4 \cdot nH_2O$, and 18-crown-6 in 1,4-dioxane furnished biaryls in good yields. Here, naphthyl- and thienylboronic acids were also used as substrates (Scheme **5.5**) [31].

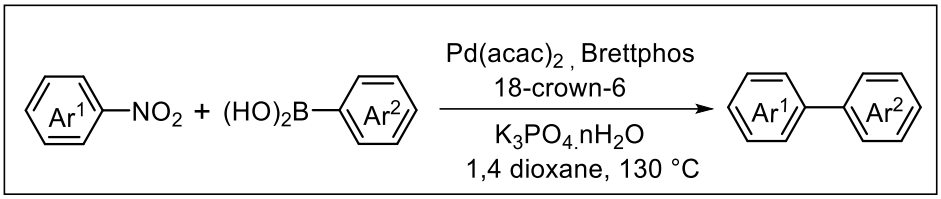

Scheme **5.5** Denitrative Suzuki–Miyaura cross-coupling reaction

5.1.5.2 Denitrative methylation

Recently, You's group developed a denitrative methylation of nitroarenes by using trimethylboroxine (TMB) as the methylating source (Scheme **5.6**). The reaction was performed in presence of Pd-BrettPhos as catalyst and Cs_2CO_3 as base. Various nitroarenes including heteroaromatics underwent methylation to give the cross-coupled product [32].

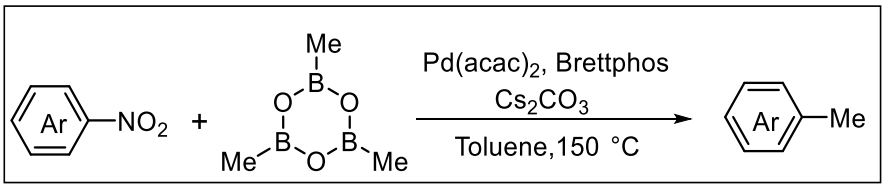

Scheme **5.6** Denitrative methylation of nitroarenes by using trimethylboroxine (TMB)

5.1.5.3 Denitrative amination

Nakao and co-workers reported a Buchwald–Hartwig amination of nitroarenes using $Pd(acac)_2$-BrettPhos as catalyst and K_3PO_4 as base (Scheme **5.7**). Nitroarenes reacted with amines to give aniline and its derivatives in good to moderate yields. Nitroarenes bearing electron-donating and electron-withdrawing substituents afford to give the corresponding aryl amines in good yields [33].

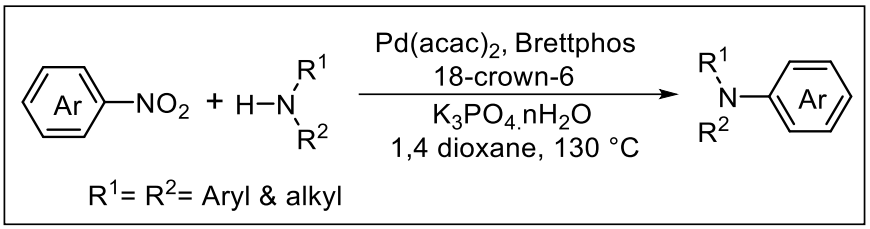

Scheme **5.7** Denitrative amination reaction

5.1.5.4 Denitrative Sonogashira coupling

In 2020, Yang group discovered a Pd-catalysed denitrative Sonogashira coupling between nitroarenes and terminal alkynes (Scheme **5.8**). They found that [Pd(en)(NO_3)$_2$] as a palladium source and BrettPhos as ligand with Cs_2CO_3 as base provided alkynes in good yields. Other than nitroarenes, heteroarenes also coupled under the optimized conditions. Silyl and alkyl alkynes were also suitable for the reaction [34].

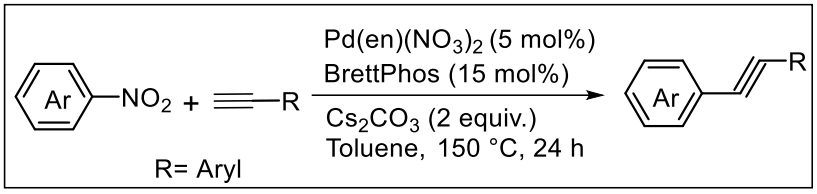

Scheme **5.8** Denitrative Sonogashira cross-coupling reaction

5.1.5.5 Denitrative Mizoroki–Heck reaction

Yamaguchi and co-workers developed a Pd-catalysed denitrative Mizoroki–Heck reaction through Pd/BrettPhos/Rb_2CO_3 catalysis (Scheme **5.9**)**.** Interestingly, the use of Rb_2CO_3 as the base and $PhCF_3$ as the solvent improved the reaction efficiency. Nitroarene possessing reactive functional groups such as esters and amines, or nitroheteroarenes, coupled with styrene derivatives to give the corresponding aryl alkenes [35].

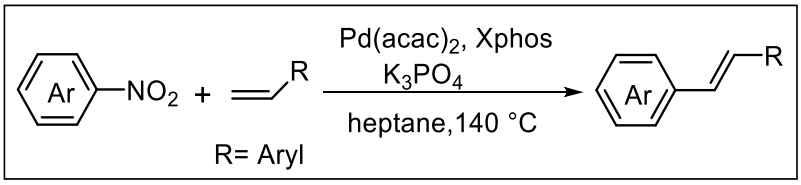

Scheme **5.9** Denitrative Mizoroki–Heck cross-coupling reaction

5.1.6 Heterogeneous metal catalyst

In 2015, United Nations outlined a sustainability development plan entitled "Transforming Our World: The 2030 Agenda for Sustainable Development" comprising of 17 sustainable development goals that addressed a broad range of topics, mainly recognizing the need for green and sustainable chemistry and engineering. The term green chemistry has been defined by IUPAC as "the invention, design and application of chemical products and processes to reduce or to eliminate the use and generation of hazardous substances'' [36]. Industrial applications of Pd as homogeneous catalysts for coupling reactions remain challenging because of high cost of palladium complexes, difficulty in separation, metal leaching of expensive catalysts, make them difficult to be used in large scale chemical processes. To overcome these difficulties and make the process more environmentally benign and economical, researchers are focusing on preparing heterogeneous palladium catalysts. Recently, heterogeneous metal catalyst has been gaining much attention due to its superior catalytic activity and selectivity [37]. Generally, heterogeneous cross-coupling reactions consist of a metal dispersed on a solid support such as carbon, magnetic materials, silica, zeolites, metal organic frameworks (MOF), organic polymers, clay minerals as well as bio-based supports (Scheme **5.10**). Moreover, heterogeneous catalyst based transformation are considered non-hazardous and greener due to its sustainability and economic viability [38]. Over the years, there has been a growing interest in the use of metal NPs on a solid support as catalysts due to their better performance and cost-effectiveness. NPs have become one of the most interesting forms of heterogeneous catalysts in cross-coupling reactions because they bear the highest surface area, offering many catalytic active sites per unit volume as compared to their bulk counterparts. However, their use has been limited by the lack of efficient separation procedures, susceptible to oxidation, resulting in complicated work up procedures in an attempt to avoid deactivation [39]. Furthermore, NPs are also prone to agglomeration or sintering upon heating [40]. Thereby, depositing metal NPs on the surface of insoluble solid supports help overcome these disadvantages. Since supports and nanocatalysts bear a high surface area, even small amounts of dispersed metal NPs on the support can lead to higher efficiency when compared to

their bulk counterpart [41]. Immobilization or encapsulation of active nanometals on a solid support helps or further slows down their tendency to undergo agglomeration [39]. Clearly, there is an urgent need to efficiently heterogenize metal catalytic species to avoid or limit the use of expensive and non-reusable homogeneous metal catalysts and obtain selective and reusable solid catalysts [42].

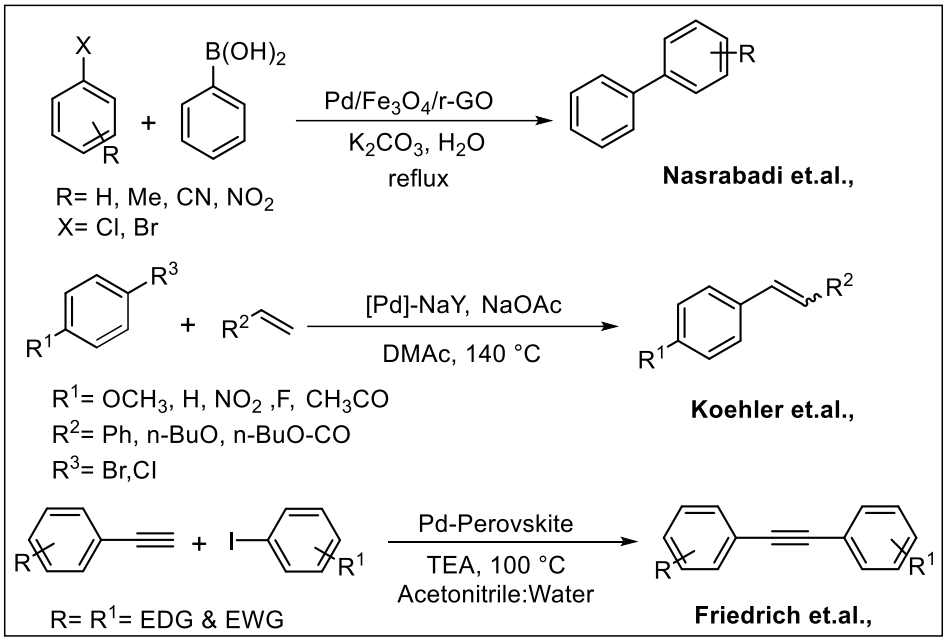

Scheme **5.10** Heterogeneous palladium catalytic system for cross-coupling reactions

During the last decade, tremendous efforts have been made towards the development of highly active and sustainable supported Pd-NPs catalysts [43,44]. Several reactions containing Pd(0) on solid support have displayed outstanding catalytic activity in cross-coupling reactions. Nasrabadi et al., reported Pd NPs supported on magnetic Fe_3O_4/reduced-graphene oxide an efficient and recoverable catalyst for Suzuki-Miyaura cross-coupling reaction (Scheme **5.10**). The heterogeneous magnetic Pd/Fe_3O_4/r-GO catalyst exhibited high catalytic activity in the Suzuki-Miyaura cross-coupling reaction in water. A series of biaryl derivatives from the reaction of phenyl boronic acid with aryl bromide or chloride derivatives were obtained in moderate to excellent yield [45]. Another [Pd]-exchanged NaY zeolites as heterogeneous catalysts exhibited high activity and selectivity towards the Heck reaction of aryl bromides with olefins for small catalyst loading (Scheme **5.10**) [46]. Ligand free heterogeneous Pd-perovskite catalyst was reported for the

Sonogashira reaction. The catalyst was highly selective and around 99–100% yield was obtained with recyability maintained up to six cycles (Scheme **5.10**) [47].

5.1.7 Bio-based derived support for cross-coupling reactions

There are a variety of methods used for the production of transition-metal NPs dispersed on a wide range of solid supports, ranging from polymers to bio-based. It seems encouraging that the growing interest in environmental friendly experimental conditions has recently prompted researchers to explore the scope of reactions that can be synthesized from waste biomass [48]. Biomasses are attractive in terms of their biocompatibility, non-toxicity, biodegradability, and more importantly, their renewable nature. They have already been exploited in diverse areas, e.g. cosmetics, agriculture, biomedical applications, sustainable applications in chemical transformation among others [49]. Pd supported on carbonaceous supports has been widely applied in C–C cross-coupling reactions. Several cross-coupling reactions involving Pd catalysts supported on natural resources such as wood [50], cotton [51], silk fibroin [52], cellulose [53] have been published recently [54]. The presence of numerous hydroxyl groups on this biomass derived substances have been utilised for reducing the metal salts to metal NPs, thus introducing a greener approach by avoiding the use of hazardous reducing agents. Interestingly, in-depth research is underway to prepare metallic NPs on various solid supports aiming to benefit cross-coupling reactions as a more efficient and sustainable approach. Some important examples of Pd NPs supported on bio-based derived support, affording products in high yields with excellent selectivity are discussed below. Konwar and group in 2015 developed cellulose supported Pd(0) NPs catalyst using hearth wood extract of Artocarpus lakoocha Roxb-as a bioreductant for Suzuki and Heck coupling reactions in water under microwave irradiation.

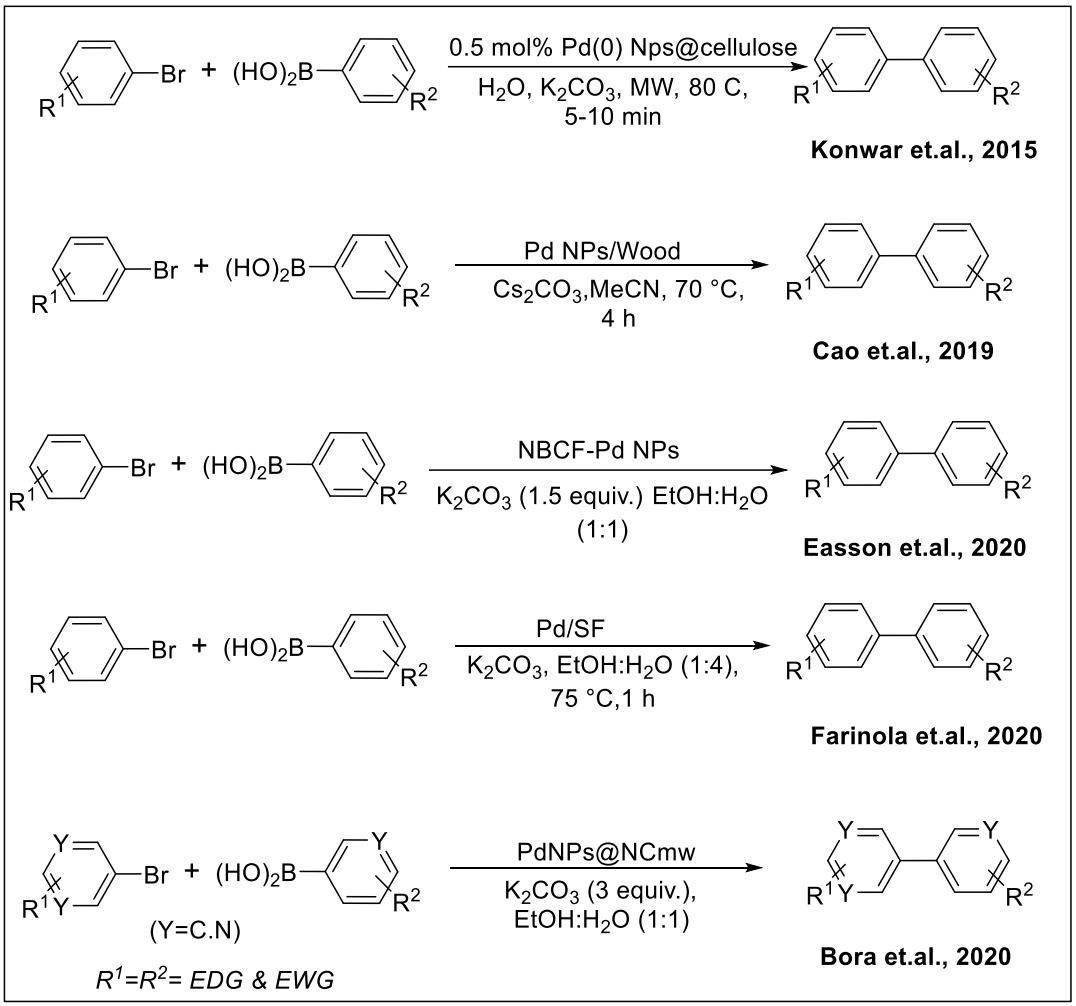

Scheme **5.11** Pd NPs on bio-based derived support for cross-coupling reaction

Pd(0) NPs@cellulose may be regarded as a very effective alternative for Suzuki and Heck reaction considering the green chemistry point of view (Scheme **5.11**) [53]. In 2019, Cao group successfully developed Pd NPs supported on the mesostructure of the hardwood (Pd NPs/wood) as a heterogeneous catalyst with the 3.5 wt% loading content of for Sonogashira, Heck and Suzuki coupling reactions. The catalyst shows good catalytic activity and could be recycled for at least five times (Scheme **5.11**) [50]. Additionally, Easson and group in 2020 developed Pd NPs deposited on nonwoven brown cotton fabric for SMC reactions. The polyphenols contained within the fabric acted as a reducing agent and the product yield obtained with this catalyst was excellent (Scheme **5.11**) [52]. Pd supported on silk fibrion (Pd/SF) as a heterogeneous catalyst was developed for SMC reaction was recently reported by Farinola and team. Pd/SF exhibited better recyclability and proceeded with low metal loading (0.38 mol%) (Scheme **5.11**) [51]. In 2021, Bora et al., developed Pd

NPs loaded onto bio-nanocellulose from cellulosic waste of pomegranate peel for Suzuki–Miyaura and Sonogashira cross-coupling reactions. The catalyst was selective and could be recycled up to five catalytic cycles without significant loss of its catalytic activity(Scheme **5.11**) [55].

5.2 Objectives of the present work

Pd-catalysed cross-coupling reactions have become most utilised methodology to synthesize C–O and C–C bonds, an important class of compounds in organic chemistry research. In this chapter, we will discuss the synthesis of Pd NPs supported on Luffa sponge (PdNPs@LS) and its catalytic performance in C–O and C–C coupling reactions.

Luffa sponge (@LS) belongs to the cucumber family; is an agriculture waste consisting of cellulose (60%), hemicellulose (30%) and lignin (10%) [56]. It is a potential precursor for preparation of carbon-based catalyst support. The rapid growth of luffa cultivation in various parts of Assam (a north-eastern state of India) has led to accumulation of luffa sponge as an agricultural waste [57]. Lignin content in luffa sponge can work as an effective reducing agent and serve to facilitate the reduction of Pd(II) to Pd(0). It can also act as a capping agent and thus helps to avoid hazardous reducing agent. Off late, natural plant-based materials have drawn tremendous attention due to cheap sources, abundance, biodegradability, non-toxicity and porous structure which facilitates the processing of greener sustainable carbon-based materials [58,59].

For the synthesis of aromatic ether, denitrative C-O bond formation method was envisioned and for that purpose, PdNPs@LS was chosen as catalyst. Interestingly, reactions involving denitrative cross-coupling are still limited in literature and needs extensive study. As aromatic ethers are important structural motif and conventional methods used for their synthesis are associated with many drawbacks, therefore search for alternative synthetic routes under sustainable approach is highly beneficial.

Next, we employed the same catalyst, PdNPs@LS for Suzuki-Miyaura cross-coupling (SMC) reaction. Over the past two decades, the SMC is considered as the most explored and powerful route for construction of C-C bonds; particularly in the

formation of biaryl motifs. Interestingly, this structural motif showed its presence in many products of commercial importance such as pharmaceuticals, natural products, polymers, fine chemicals, agrochemicals and molecular wires. Hence, to develop simple and economical methodology, the exercise of heterogeneous catalyst, ligand-free system, moderate basicity and wide compatibility have to be carried out to establish a greener and sustainable strategy (Scheme **5.12**).

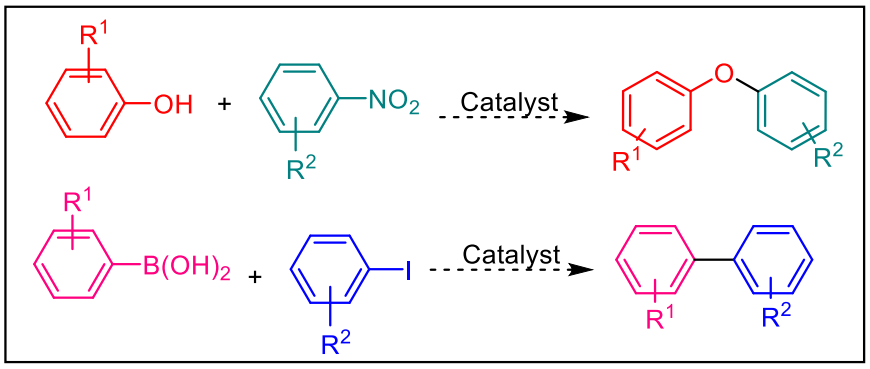

Scheme **5.12** Proposed reaction schemes of C-O and C-C coupling

5.3 Results and Discussion

5.3.1 Characterization of the catalyst

Fourier Transform-Infrared (FT-IR) Spectroscopy:

FT-IR spectra of the bio-based support and Pd supported catalyst are compared in Figure **5.2**. The observed peaks in the wavenumber range of 3660-2900 cm^{-1} are characteristic for the stretching vibration of O-H and C-H bonds in polysaccharides also attributed to the hydroxyl groups in phenolic structure of lignin. The broad peak at 3415 cm^{-1} is also the characteristic for stretching vibration of the hydroxyl group in polysaccharides. The band at 2894 cm^{-1} is identified as the C-H stretching frequency of all hydrocarbons constituted in polysaccharides. Typical bands assigned to cellulose were observed in the region of 1630-900 cm^{-1}. The peaks located at 1633 cm^{-1} correspond to the vibration of water molecules absorbed in cellulose [60,61]. Further, the peak at 597 cm^{-1} region signifies the presence of Pd(0) particles anchored on the luffa sponge [62].

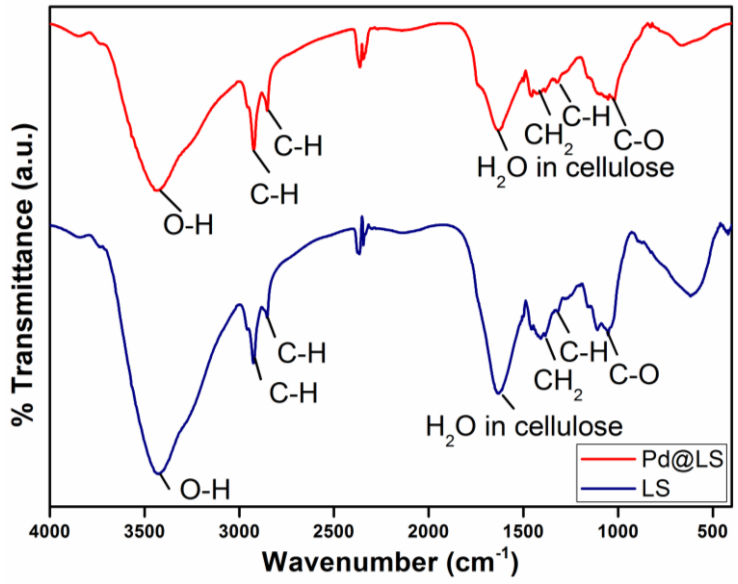

Figure **5.2** FTIR spectra of LS and PdNP@LS

Thermo-Gravimetric (TGA) analysis:

TGA was carried out for the bio-based supported metal catalyst to comprehend its thermal stability. During the process of TGA analysis, the very first weight loss (0.15 mg) was observed between the temperature range 49.3-124.3 °C which corresponds to the removal of water as well as volatile organic materials. However, the majority of degradation was observed between 192.7-285.3 °C (0.83 mg). This corresponds to the disintegration of the hemicelluloses/cellulose content of the support [63].

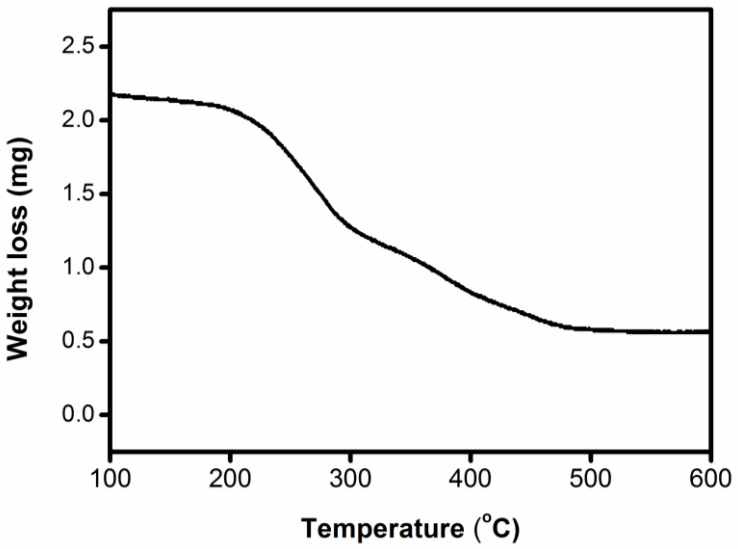

Figure **5.3** TGA of Pd NPs@LS

Again, a third phase of degradation was seen between 312.9 - 394.8 °C which led to 0.34 mg of weight loss indicating that the support lost its lignin content. No significant weight loss was seen above 600 °C. This is mainly because of the existence of inert carbon atoms; which are usually unaltered at higher temperatures (Figure **5.3**) [64].

Powder X-Ray Diffraction (p-XRD) analysis:

The crystalline nature of the synthesized PdNPs@LS was determined using the powder X-ray diffraction technique. Easy distinction can be made from the p-XRD pattern shown in Figure **5.4**. The observed intense peaks at 2θ (40, 46, 68) correspond to crystallographic planes (111), (200) and (220) fcc lattice planes of Pd respectively, with *d* spacing values 0.23 and 0.19 nm respectively [65]. Further, the p-XRD pattern matches well with JCPDS card No. 05-0681, confirming the successful formation of Pd NPs [66].

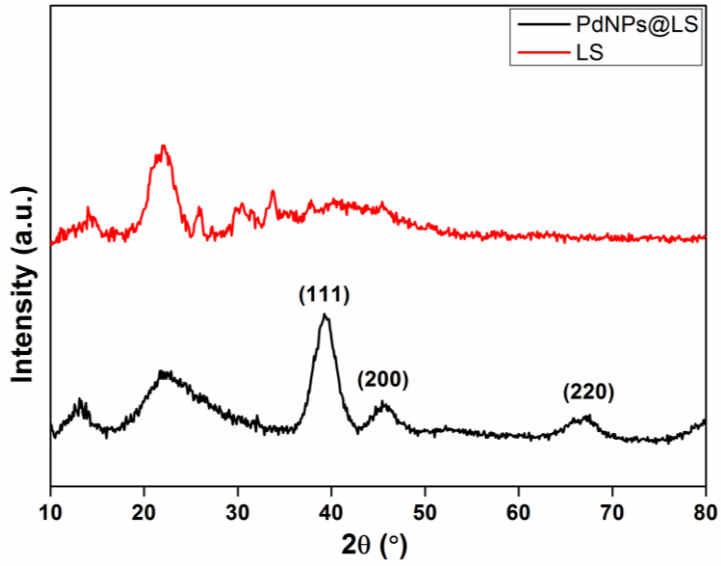

Figure **5.4** Powder XRD patterns of @LS and PdNPs@LS

Scanning electron microscopy-energy dispersive X-ray (SEM-EDX) analysis: SEM analysis has depicted the particle structure and surface morphology of the obtained bio-based supported PdNPs@LS catalyst. The surface (20 µm) shows rough and uneven pores, with highly irregular surface [Figure **5.5**(**a**)]. Energy dispersion X-ray spectroscopy (EDX) was recorded as shown in [Figure **5.5**(**b**)]. The

observed peak assigned to palladium metal in EDX spectrum, shows the successful presence of palladium metal.

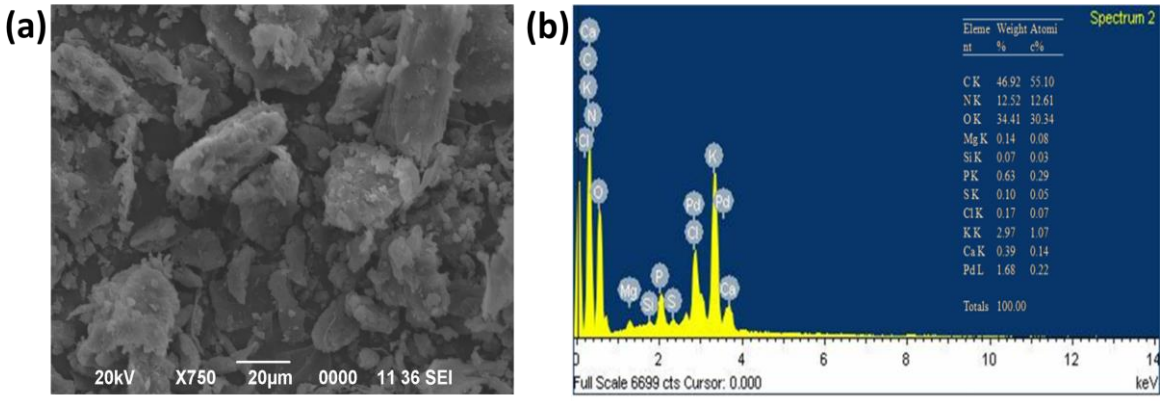

Figure **5.5** (a) SEM and (b) EDX images of PdNPs@LS

Transmission Electron Microscopy (TEM) analysis:

The morphology of the *in situ*-generated PdNPs@LS was studied by TEM analysis. It can be seen from the TEM image that the interplanar distance of 0.22 nm and 0.19 nm correspond to the lattice planes (111) and (200) respectively [Figure **5.6**(a,b)]. The TEM images also clearly reflects crystalline fringes with three well-resolved rings as indexed in the selected area electron diffraction (SAED) pattern of the PdNPs in [Figure **5.6** (**c**)]. The crystal lattice planes as depicted namely (111), (200) and (220) agree well with the p-XRD database suggesting the fcc crystal structure of the PdNPs [55,67]. Additionally, it is observed that the PdNPs are well dispersed and are spherical in shape. The distribution of the *in situ*-generated Pd NPs was analyzed and the resultant data were plotted in a histogram showing a majority of particles being in the range of 20-40 nm [Figure **5.6**(**d**)]. Thus, the p-XRD pattern further substantiates the highly crystalline nature of NPs observed from SAED pattern depicting concentric rings [66].

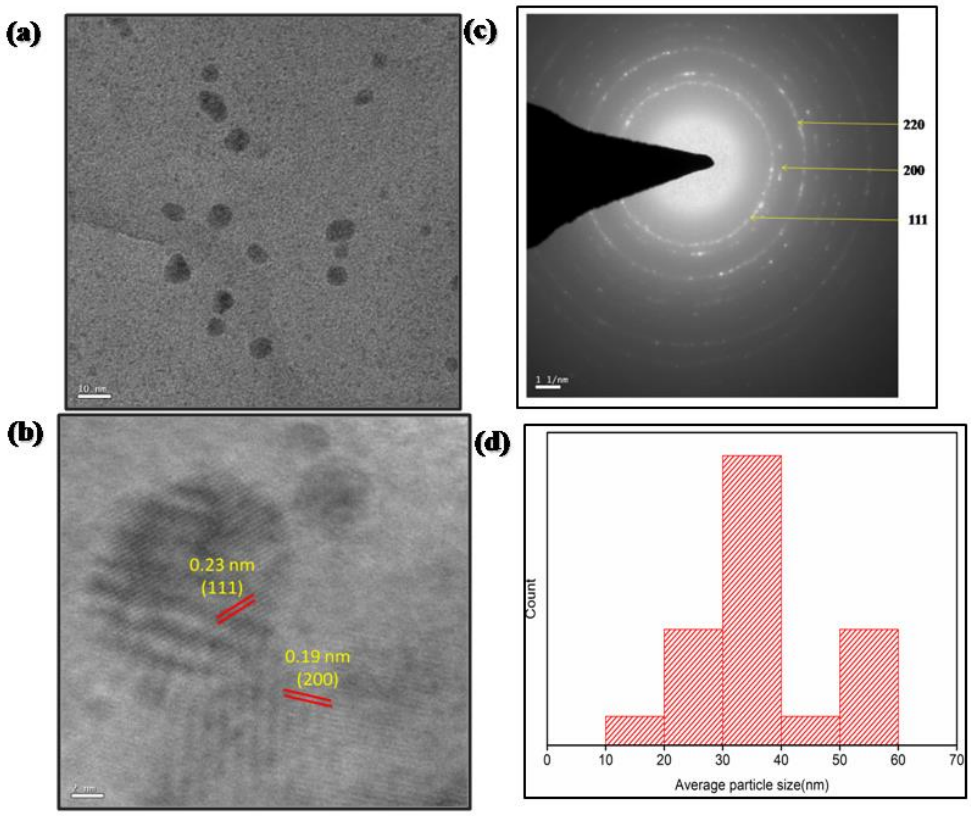

Figure **5.6** TEM images of (a) PdNPs@LS; (b) HRTEM image showing lattice fringes; (c) SAED pattern; and (d) particle size distribution histogram of PdNPs@LS.

X-ray photoelectron spectroscopy (XPS) analysis:

The elemental composition and the chemical bonding of PdNPs@LS were recorded using X-ray photoelectron spectroscopy (XPS) (Figure **5.7**). The XPS survey spectrum of PdNPs@LS was found to contain three sharp peaks at 285.07, 336.13, and 532.36 eV which signify the presence of C1s, Pd3d and O1s electrons respectively, indicating the successful synthesis of PdNPs@LS catalyst. The high resolution spectrum of O1s was fitted with one distinct peak at 531.15 eV attributed to the C-OH bond. The deconvoluted high resolution spectrum of C1s contains three sharp peaks with binding energy values 284.77, 286.36, and 288.14 eV which can be assigneto C-C, C-OH, and C=O bonds of PdNPs@LS respectively.

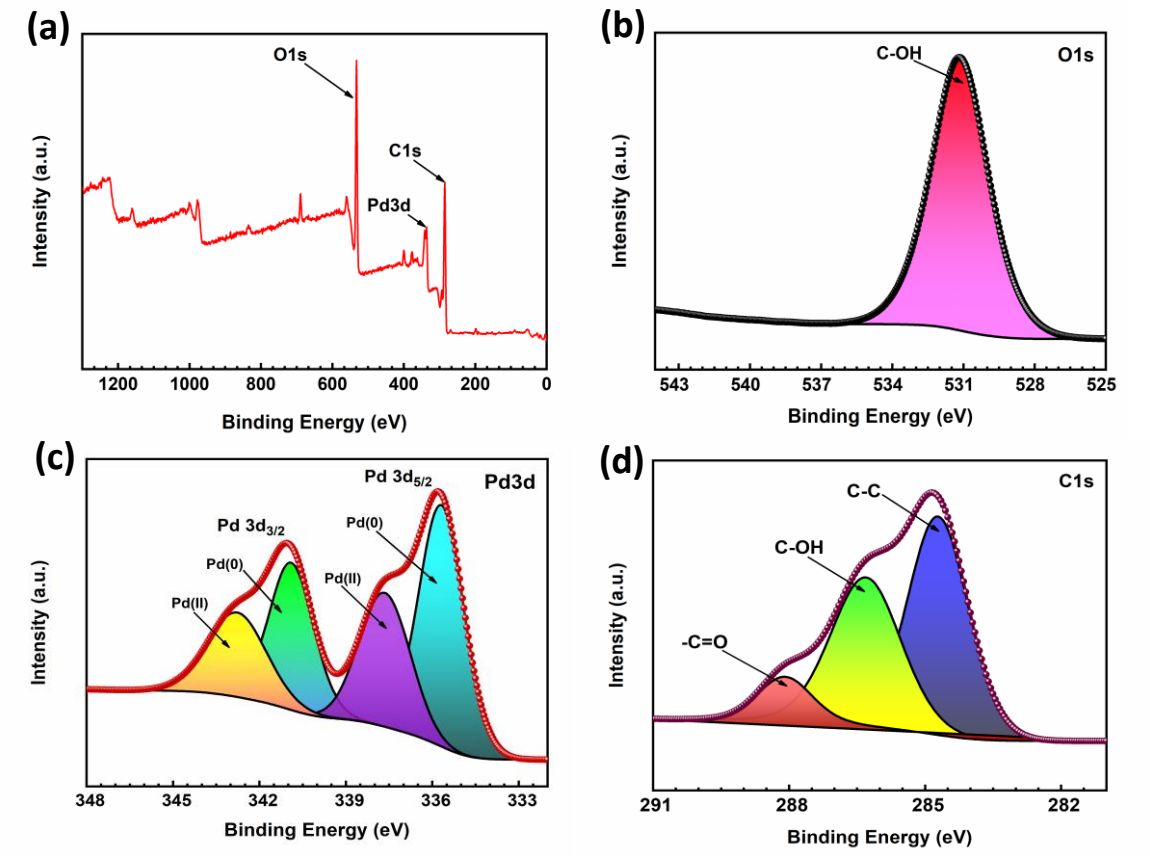

Figure **5.7** XPS spectra of (a) Survey plot and high resolution XPS spectra (b) O1s, (c) Pd3d, and (d) C1s of PdNPs@LS.

The high-resolution spectrum of Pd3d core level spectrum of PdNPs@LS nanocomposite shows two binding energy values at 335.68 and 341.03 eV for Pd $3d_{3/2}$ and Pd $3d_{5/2}$, respectively which confirms the formation of Pd (0) NPs. The satellite peaks at 337.65 and 342.77 eV corresponding to the Pd $3d_{3/2}$ and Pd $3d_{5/2}$, respectively confirm that Pd (II) species were also present in the PdNPs@LS nanocomposites [55].

5.3.2 Application of the catalyst in diaryl ether synthesis

5.3.2.1 Optimization Study

Table **5.1** Optimization of reaction conditions[a]

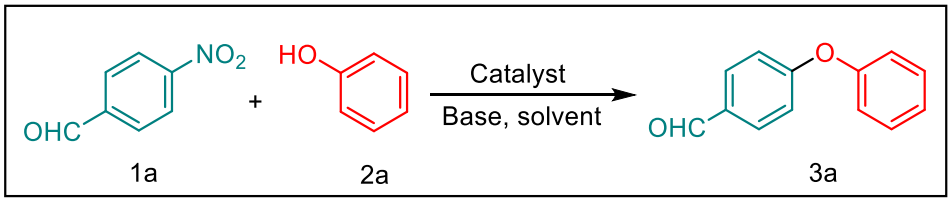

Entry	Amount of catalyst (wt%)	Solvent (mL)	Base (1 equiv.)	Time (h)	Yield(%)[b] 3a
1	5	DMSO	K_2CO_3	12	71
2	10	DMSO	K_2CO_3	12	87
3	15	DMSO	K_2CO_3	12	89
4	**10**	**DMSO**	**K_2CO_3**	**6**	**88**
5	10	DMAc	K_2CO_3	6	67
6	10	CAN	K_2CO_3	6	47
7	10	EtOH	K_2CO_3	6	nr
8	10	H_2O	K_2CO_3	6	nr
9	10	DMSO	Et_3N	6	nr
10	10	DMSO	NaOH	6	37
11	10	DMSO	-	6	nr

[a]Reaction Conditions: ***1a*** *(0.5 mmol),* ***2a*** *(0.5 mmol), and solvent (3 mL).* [b]*Isolated yields. nr= no reaction*

After careful observation and confirmation of the synthesised PdNPs@LS, we attempted to find a suitable reaction condition for diaryl ether synthesis. To study the effectiveness of the catalyst, 4-nitrobenzaldehyde and phenol were chosen as model substrates. The reaction conditions were optimised in terms of the catalyst loading, base, reaction time, temperature and solvent. It is worth mentioning that the system showed good catalytic activity for coupling of various substituted benzaldehydes and phenols in DMSO. An initial screening of the effect of different solvents such as DMSO, DMAc, ACN, ethanol and H_2O (Table **5.1,** entries 4-8) were done where DMSO was seen as the most effective one with 88% yield (Table **5.1,** entry 4). The presence of 1equiv. K_2CO_3 was essential as the reaction does not proceed in absence of base (Table **5.1,** entry 11). Lower yield of the product was obtained in presence of NaOH (Table **5.1,** entry 10) and unfortunately no product was obtained with organic base Et_3N (Table **5.1,** entry 9). Next, we optimized the reaction condition for different amount of catalyst (5, 10, 15 wt%) and found that 10 wt% of PdNPs@LS (Table **5.1,** entries 1-4) gave the best result. Thus, the best reaction conditions for the formation of biaryl ethers were fixed at 10 wt% of PdNPs@LS as catalyst in DMSO solvent, 1 equiv. of K_2CO_3 as base at 100 °C (Table **5.1,** entry 4).

5.3.2.2 Substrate scope study

To evaluate the scope and limitation of the catalyst, we examined variations in both the coupling partners. Using 4-nitrobenzaldehyde, a variety of phenols was analyzed. Phenols bearing methyl, *tert*-butyl, formyl, chloro, bromo, substituents (Table **5.2**, entries 3b-3e, and 3i) were well tolerated as shown by the formation of ethers. Products derived from electron-deficient phenols provided slightly lower yields compared to electron donating phenols (Table **5.2**, entries 3d, 3e and 3i). Substituted nitroarenes such as 4-formyl, 4-chloro, 4-cyano also offered good yield of the product (Table **5.2,** entries 3a-3i).

Table **5.2** Substrate scope study[a]

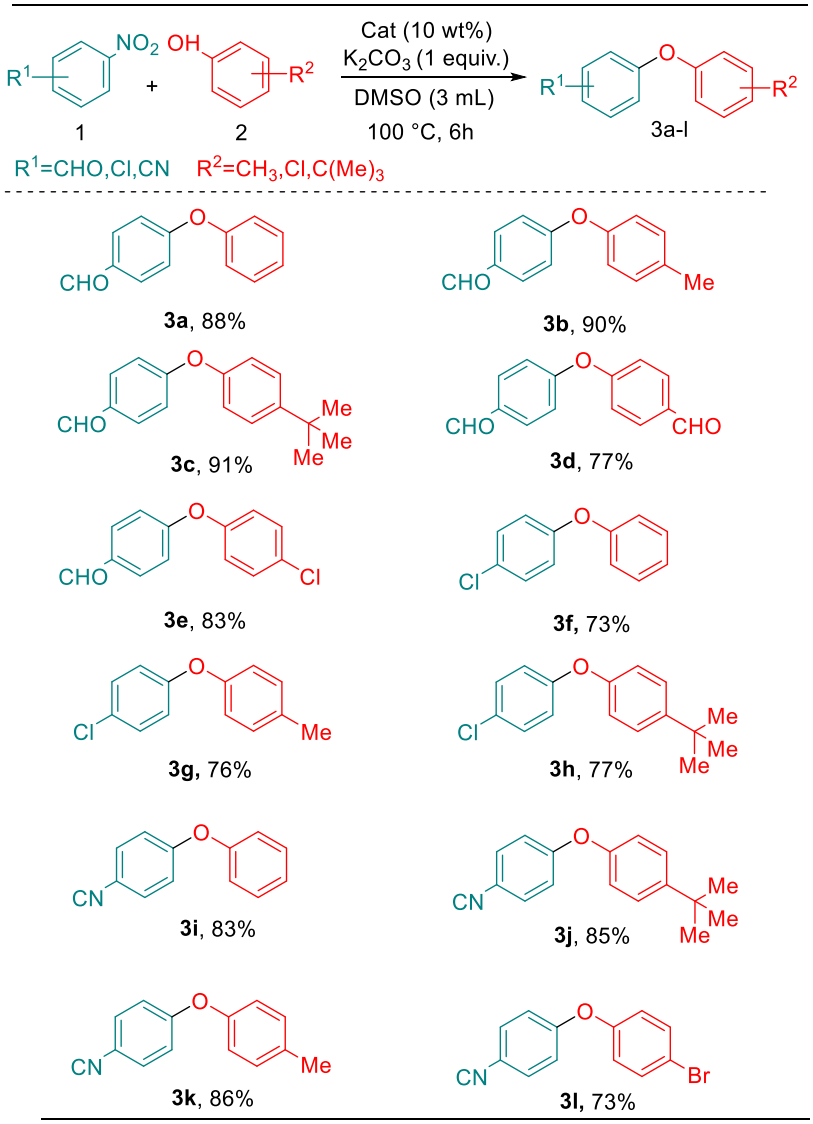

[a]Reaction Conditions: ***1*** *(0.5 mmol),* ***2*** *(0.5 mmol), catalyst (10 wt%) and solvent (3 mL).*

5.3.2.3 Mechanism

The mechanism of the denitrative ether synthesis by palladium was well established through the comprehensive studies by the research group of Bora [29]. The oxidative addition of the nitroarene to the Pd surface favours their extraction to yield ArPd(II)NO_2 moieties in solution and thus it is this species that ultimately furnishes the product and generates free Pd(0) to undergo the catalytic cycle again as shown in Figure **5.8.**

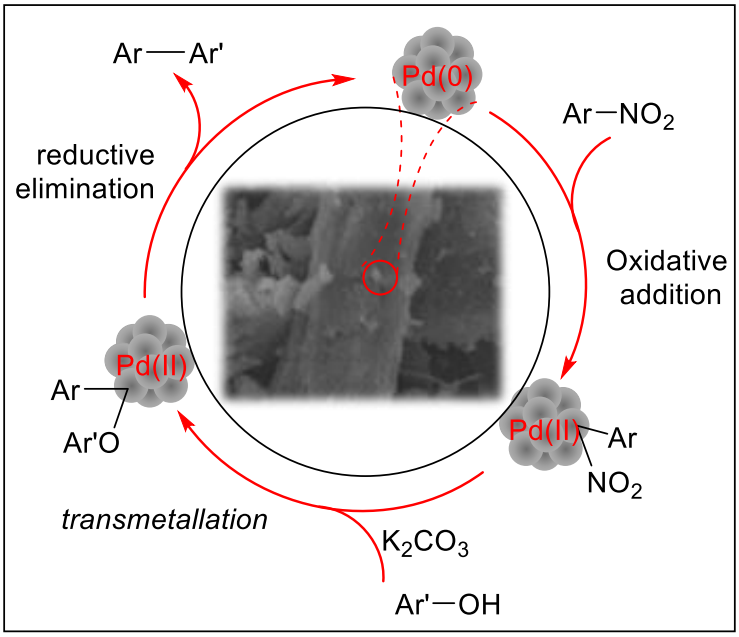

Figure **5.8** Plausible Mechanism for denitrative C-O bond formation

5.3.3 Application of the catalyst in the Suzuki–Miyaura cross-coupling reaction

5.3.3.1 Optimization Study

To investigate the catalytic activity of PdNPs@LS towards the SMC reaction, the efficiency of this catalyst was initially assessed for 4-Methoxyiodobenzene and phenylboronic acid with 5 wt% catalyst using K_2CO_3 as base and EtOH:H_2O as solvent at 60 °C for 12 h (Table **5.3**). Among the different bases studied, such as K_2CO_3, NaOH, Et_3N (Table **5.3**, entries **1** and **10-13**); K_2CO_3 suited the best among all tested bases in terms of reaction time and efficiency (Table **5.3**, entry **3**). We have also performed the reaction in different solvents such as EtOH, CH_3CN, *i*-PrOH, H_2O, EtOH:H_2O (Table **5.3**, entries **1** and **7–11**). Among all, EtOH:H_2O solvent system

served to be an efficient reaction medium and delivered the desired product at 60 °C in 8 h reaction time (Table **5.3**, entry **3**). The yield of the product obtained was maximum at 60 °C and no further increase in product yield was observed with increasing temperature. We also discovered that the presence of water was critical for the reaction to yield good results. Also, the increase in the catalyst amount from 10 wt% to 15 wt% did not show any significant improvement in the product yield (Table **5.3**, entries **3** and **4**). Thus, 10 wt% PdNPs@LS was sufficient for the present Suzuki–Miyaura coupling reactions (Table **5.3**, entry **1**). It was found that the reaction went to completion in 8 h (Table **5.3**, entries **1-3**), and prolonging the reaction time could not increase the yield. The general applicability of the Suzuki reaction catalysed by PdNPs@LS was tested for various aryl iodides and substituted phenyl boronic acid under the optional conditions;10 wt% PdNPs@LS and K_2CO_3 (2 equiv.) in EtOH:H_2O (1:1) (4mL) at 60 °C for 8 h and the results are depicted in Table **5.3.**

Table **5.3 Optimization of reaction conditions**[a]

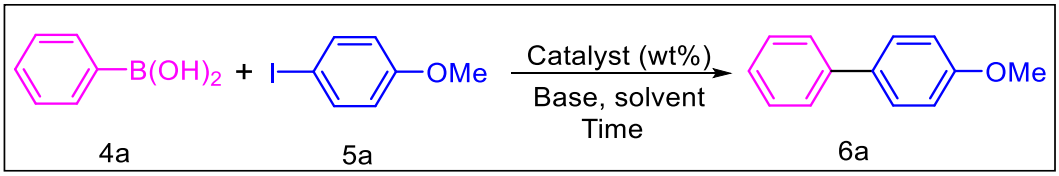

Entry	Catalyst (wt%)	Base (2 equiv.)	Solvent (mL)	Time (h)	Yield (%)[b] 6a
1	5	K_2CO_3	EtOH:H_2O (1:1)	12	81
2	10	K_2CO_3	EtOH:H_2O (1:1)	12	90
3	**10**	**K_2CO_3**	**EtOH:H_2O (1:1)**	**8**	**90**
4	15	K_2CO_3	EtOH:H_2O (1:1)	8	91
5	10	K_2CO_3	EtOH	12	73
6	10	K_2CO_3	H_2O	12	61
7	10	K_2CO_3	CH_3CN	8	59
8	10	K_2CO_3	*i*-PrOH	8	57
9	10	K_2CO_3	1,4-Dioxane	8	47
10	10	Na_2CO_3	EtOH:H_2O (1:1)	8	89
11	10	NaOH	EtOH:H_2O (1:1)	8	53

12	10	Et_3N	EtOH:H_2O (1:1)	8	43
13	10	Cs_2CO_3	EtOH:H_2O (1:1)	8	87
14	-	K_2CO_3	EtOH:H_2O (1:1)	8	nr

*[a]Reaction Conditions: **4a** (0.5 mmol), **5a** (0.75 mmol), temp. (60 °C) and solvent (3 mL).[b]Isolated yields, nr= no reaction*

5.3.3.2 Substrate scope study

The reaction of a wide variety of aryl halides and boronic acids was examined using optimized conditions and the results are shown in Table **5.4**. The catalytic system was studied for electronically diverse aryliodides and arylboronic acid.

Table **5.4 Substrate scope study**[a]

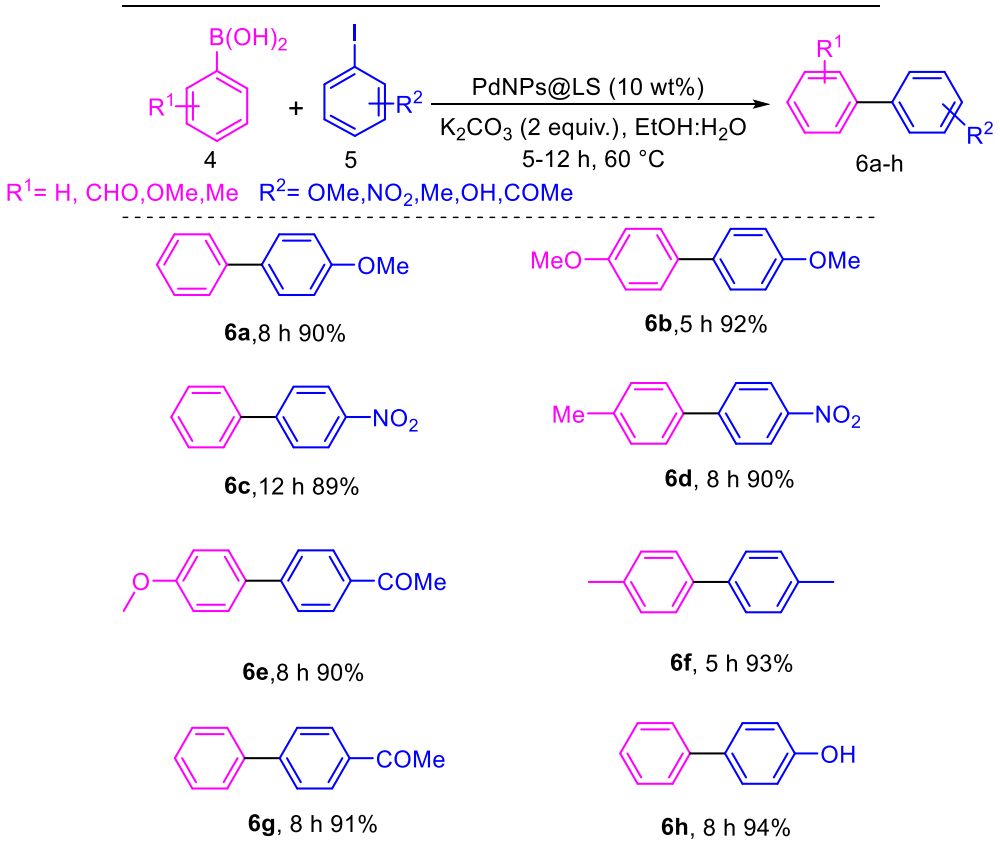

[a]Reaction Conditions: **4** (0.5 mmol), **5** (0.65 mmol), catalyst (10 wt%), base (2 equiv.), solvent (3 mL).

No significant change was noticed with electronically diverse substituents in the reaction. Both aryl iodides and arylboronic acids with electron-donating and

electron-withdrawing substitutions exhibited similar activity and the corresponding biphenyl compounds were produced in good to excellent yields in 8 h reaction time (Table **5.4** entries 6a-6h). From Table **5.4**, it was observed that electronically varied arylboronic acid did not affect the product yield. The results demonstrated that PdNPs@LS was an effective catalyst for Suzuki coupling reactions of arylboronic acids with aryl iodides.

5.3.3.3 Mechanism

The mechanism of the SMC reaction was well established through comprehensive studies by the research group of Feliu Maseras [68]. It is well-known that Suzuki-Miyaura cross-coupling reactions follow a well-defined catalytic cycle based on three crucial steps: i) oxidative addition of the organic halide to the Pd(0) complex to give Ar-Pd(II)-I; ii) transmetalation between the Ar-Pd(II)-I and the phenyl boronic acid Ar'-$B(OH)_2$ with the assistance of a base; and finally, iii) reductive elimination to form a new C–C bond, Ar-Ar' with the simultaneous regeneration of the catalyst as shown in (Figure **5.9**).

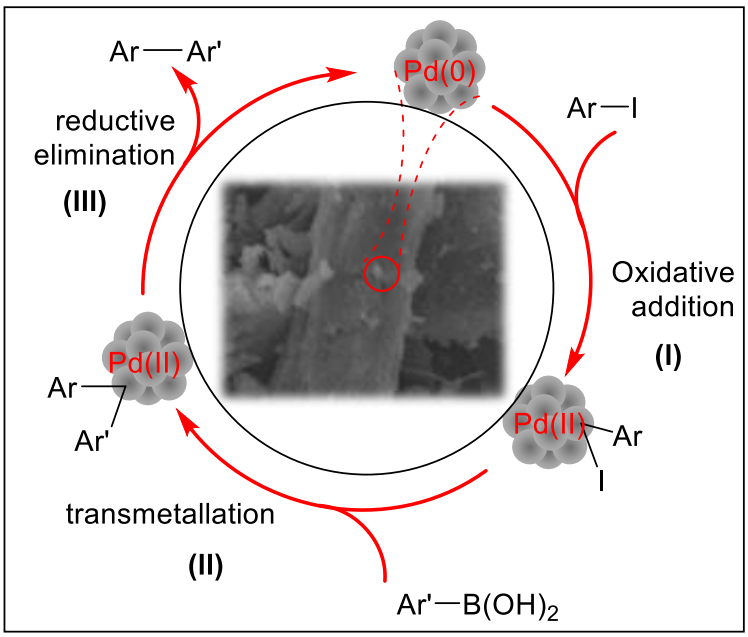

Figure **5.9** Plausible mechanism for SMC reaction

5.3.4 ICP-OES analysis and screening of recyclability of the catalytic system

Recyclability of catalyst in a reaction protocol is essential for commercial applications from the standpoint of cost-effectiveness and environmental impact. The reusability of the catalyst was investigated for the synthesis of diarylethers and SMC reaction under the optimized reaction conditions. Palladium content on the surface of support was quantified using ICP-OES analysis. Analysis showed that the Pd content was 19 mg gm^{-1}. The reaction runs over three consecutive runs with excellent to moderate quantitative yields, revealing the practical recyclability of the catalyst (Figure **5.10**). A slight loss in reactivity after repeated use was probably due to physical loss of the catalyst.

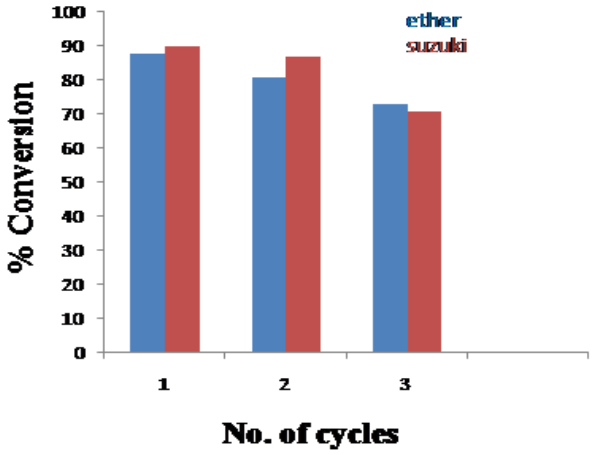

Figure **5.10** Recyclability of PdNPs@LS over three cycles

5.4 Conclusion

In conclusion, we have demonstrated that the heterogeneous palladium catalyst PdNPs@LS is a highly efficient catalyst for the synthesis of diarylethers and Suzuki-Miyaura cross-coupling reaction. The catalyst was characterized by FT-IR, TGA, p-XRD, SEM-EDX, TEM, XPS and ICP-OES analyses. This simple synthetic method has the advantages of high product yields, easy preparation, biodegradable support, simple work-up procedure, and easy handling of the catalyst. Thus, the newly synthesized PdNPs@LS is robust, selective which can be recovered and reused without any significant loss of activity.

5.5 Experimental section

5.5.1 Experimental procedure

Preparation of Catalyst: It is known that lignin content in luffa sponge could work as an effective reducing reagent to reduce Pd(II) to Pd(0). The Pd NPs supported on the luffa sponge were prepared *in-situ* by heating 1gm of the crushed luffa sponge added into 25 mg palladium acetate, $Pd(OAc)_2$ and refluxed in ethanol for 12 h at 60 °C. After 12h, the colour of the crushed luffa sponge turned from its natural yellow to black. The PdNPs supported on luffa sponge was cooled and centrifuged at 4000 rpm and then washed thoroughly with ethanol followed by drying in vacuum.

General procedure for synthesis of aromatic ethers from substituted nitroarenes and phenols: In a 50 mL round bottomed flask, a mixture of nitrobenzaldehyde (**1**, 0.5 mmol), substituted phenols (**2**, 0.5 mmol), K_2CO_3 (1equiv.) and catalyst (10 wt%) was added and stirred in DMSO (3 mL) and refluxed for 6 h. The progress of the reaction was monitored by TLC and upon completion, the reaction mixture was worked up, the product was isolated, and catalyst was washed and separated by centrifugation with ethanol and dried under vacuum. The catalyst was further reused and the products (**3a-l**) were purified using column chromatography with silica gel (60-120 mesh) and ethylacetate-hexane as eluent system.

General procedure for synthesis of biaryl derivatives from phenylboronic acids and aryl iodides: Aryl halide (**4**, 0.5 mmol), arylboronic acid (**5**, 0.65 mmol), K_2CO_3 (2 equiv.), PdNPs@LS (10 wt%), and EtOH:H_2O (1:1) (4mL) were taken in a 50 mL round bottomed flask and the reactants were stirred at 60 °C. After completion of the reaction, the catalyst was separated from the reaction mixture by centrifugation and the crude reaction mixture was extracted with ethyl acetate (3 × 10 mL). The resultant organic phase was washed and dried over anhydrous Na_2SO_4, filtered and evaporated under reduced pressure, and products (**6a-h**) were purified by column chromatography using ethyl acetate and *n*-hexane as eluents. The products were characterized by ^1H and ^{13}C NMR spectroscopic analyses.

5.5.2 Characterisation data of the products

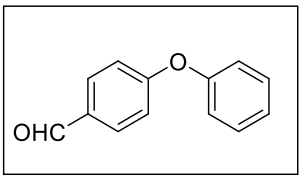

4-phenoxybenzaldehyde (**3a**)

White solid (87.21 mg, 88%); ^{1}H NMR (400 MHz, $CDCl_3$) δ (ppm) 9.85 (s, 1H), 7.77 (d, J = 8.6 Hz, 2H), 7.34 (t, J = 8.0 Hz, 2H), 7.15 (t, J = 7.5 Hz, 1H), 7.00 (dd, J = 11.0, 8.4 Hz, 4H); ^{13}C NMR (100 MHz, $CDCl_3$) δ (ppm) 190.8, 163.3, 155.1, 131.9, 131.3, 130.1, 125.0, 120.4, 117.6.

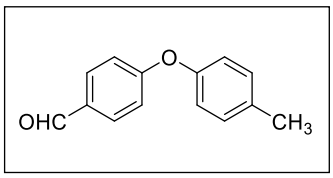

4-(p-Tolyloxy)benzaldehyde (**3b**)

Off white solid (95.51 mg, 90%); ^{1}H NMR (500 MHz, $CDCl_3$) δ (ppm) 9.91 (s, 1H), 7.83 (d, J = 8.2 Hz, 2H), 7.21 (d, J = 8.0 Hz, 2H), 7.01 (dd, J = 26.7, 8.1 Hz, 4H), 2.37 (s, 3H); ^{13}C NMR (125 MHz, $CDCl_3$) δ (ppm) 190.8, 163.7, 152.7, 134.7, 131.9, 131.05, 130.7, 120.4, 117.2, 20.8.

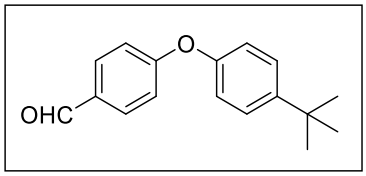

4-(4-(tert-Butyl)phenoxy)benzaldehyde (**3c**)

Brown solid (115.72 mg, 91%); ^{1}H NMR (400 MHz, $CDCl_3$) δ (ppm) 9.90 (s, 1H), 7.85–7.79 (m, 2H), 7.44–7.38 (m, 2H), 7.07–6.97 (m, 4H), 1.33 (s, 9H); ^{13}C NMR (100 MHz, $CDCl_3$) δ (ppm) 190.9, 163.7, 152.6, 148.1, 132.0, 131.1, 127.1, 120.0, 117.4, 34.6, 31.6.

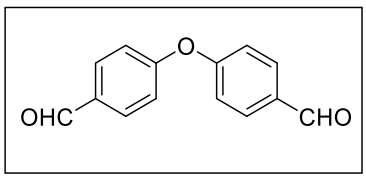

4,4'-Oxydibenzaldehyde (**3d**)

Yellow solid (87.1 mg, 77%); ^{1}H NMR (500 MHz, $CDCl_3$) δ (ppm) 9.98 (s, 2H), 7.97–7.89 (m, 4H), 7.21–7.14 (m, 4H); ^{13}C NMR (125 MHz, $CDCl_3$) δ (ppm) 190.7, 161.0, 132.7, 132.1, 119.4.

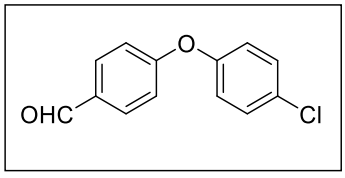

4-(4-Chlorophenoxy)benzaldehyde (**3e**)

White solid (96.55 mg, 83%); ^{1}H NMR (500 MHz, $CDCl_3$) δ (ppm) 10.00 (s, 1H), 8.28 (d, J = 9.2 Hz, 2H), 7.96 (d, J = 8.7 Hz, 2H), 7.17 (dd, J = 30.9, 8.9 Hz, 4H);

^{13}C NMR (125 MHz, $CDCl_3$) δ (ppm) 190.6, 161.3, 160.4, 143.8, 133.1, 132.2, 126.1, 119.8, 118.9.

1-Chloro-4-phenoxybenzene (**3f**)

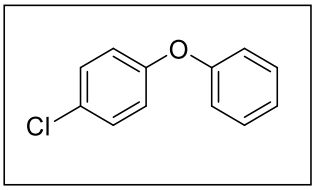

Brown solid (74.69 mg, 73%); ^{1}H NMR (500 MHz, $CDCl_3$) δ (ppm) 8.23–8.14 (m, 2H), 7.47–7.39 (m, 2H), 7.28–7.22 (m, 1H), 7.13–6.92 (m, 4H); ^{13}C NMR (125 MHz, $CDCl_3$) δ (ppm) 163.4, 154.7, 142.7, 130.3, 125.9, 125.4, 120.6, 117.1.

1-Chloro-4-(p-tolyloxy)benzene (**3g**)

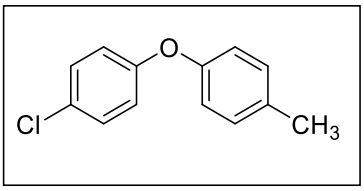

Pale yellow solid (83.09 mg, 76%); ^{1}H NMR (500 MHz, $CDCl_3$) δ (ppm) 8.23–8.14 (m, 2H), 7.23 (d, J = 8.0 Hz, 2H), 6.98 (dd, J = 8.9, 2.7 Hz, 4H), 2.38 (s, 3H); ^{13}C NMR (125 MHz, $CDCl_3$) δ (ppm) 163.7, 152.3, 142.4, 135.2, 130.8, 125.9, 120.4, 116.7, 20.8.

1-(tert-Butyl)-4-(4 chlorophenoxy)benzene (**3h**)

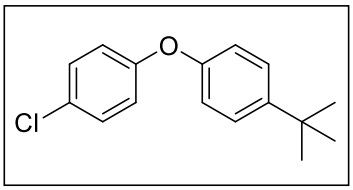

Off white solid (100.39 mg, 77%); ^{1}H NMR (500 MHz, $CDCl_3$) δ (ppm) 8.24–8.14 (m, 2H), 7.50–7.38 (m, 2H), 7.09–6.94 (m, 4H), 1.35 (d, J = 1.6 Hz, 9H); ^{13}C NMR (125 MHz, $CDCl_3$) δ (ppm) 163.7, 152.2, 148.4, 142.4, 127.1, 125.9, 120.0, 116.8, 31.4.

4-Phenoxybenzonitrile (**3i**)

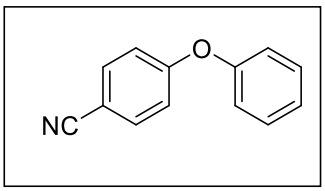

White solid (83%, 81.01 mg); ^{1}H NMR (400 MHz, $CDCl_3$) δ (ppm) 7.62–7.56 (m, 2H), 7.43–7.37 (m, 2H), 7.27–7.19 (m, 1H), 7.08–6.96 (m, 4H); ^{13}C NMR (100 MHz, $CDCl_3$) δ (ppm) 161.1, 154.1, 134.3, 133.3, 122.1, 118.7, 118.1, 118.0, 106.4.

4-(4-(tert-Butyl)phenoxy)benzonitrile (**3j**)

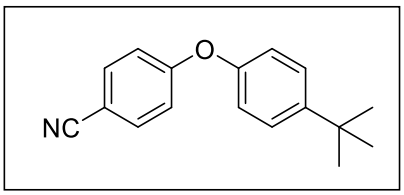

Pale white solid (86%, 106.81 mg); ^{1}H NMR (500 MHz, $CDCl_3$) δ (ppm) 7.54–7.47 (m, 2H), 7.37–7.29 (m, 2H), 6.96– 6.86 (m, 4H), 1.27 (s, 9H); ^{13}C NMR

(125 MHz, $CDCl_3$) δ (ppm) 160.9, 151.3, 147.1, 133.0, 126.0, 118.8, 117.9, 116.6, 104.4, 33.4, 30.4.

4-(p-Tolyloxy)benzonitrile (**3k**)

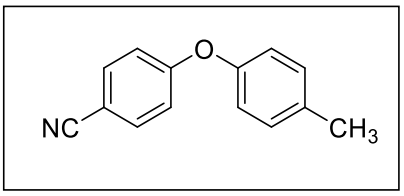

Brown solid (88.9 mg, 85%); ^{1}H NMR (500 MHz, $CDCl_3$) δ (ppm) 7.57 (dd, J = 9.0, 2.2 Hz, 2H), 7.20 (d, J = 8.0 Hz, 2H), 7.01–6.91 (m, 4H), 2.37 (s, 3H). ^{13}C NMR (125 MHz, $CDCl_3$) δ (ppm) 162.1, 152.4, 134.9, 134.1, 130.7, 120.4, 118.9, 117.6, 105.5, 20.8.

4-(4-Bromophenoxy)benzonitrile (**3l**)

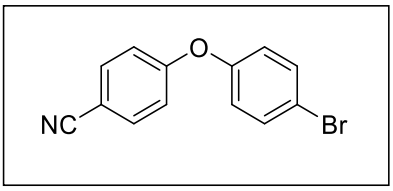

White solid (100.05 mg, 73%); ^{1}H NMR (400 MHz, $CDCl_3$) δ (ppm) 7.62–7.58 (m, 2H), 7.53–7.48 (m, 2H), 7.03–6.97 (m, 2H), 6.96–6.91 (m, 2H); ^{13}C NMR (100 MHz, $CDCl_3$) δ (ppm) 161.8, 154.9, 134.3, 130.4, 125.2, 120.6, 118.9, 118.0, 105.9.

4-Methoxy-1,1'-biphenyl (**6a**)

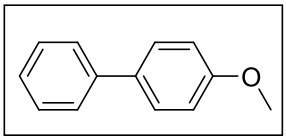

White solid (82.90 mg, 90%); ^{1}H NMR (400 MHz, $CDCl_3$) δ (ppm) 7.61 (d, J = 9.6 Hz, 4H), 7.47 (t, J = 7.6 Hz, 2H), 7.36 (d, J = 7.4 Hz, 1H), 7.03 (d, J = 8.9 Hz, 2H), 3.90 (s, 3H); ^{13}C NMR (100 MHz, $CDCl_3$) δ (ppm) 159.2, 133.8, 128.8, 128.2, 126.8, 126.7, 114.3.

4,4'-Dimethoxy-1,1'-biphenyl (**6b**)

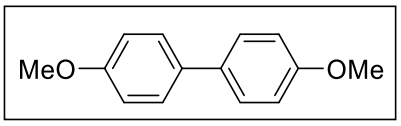

Dirty white (98.55 mg, 92%); ^{1}H NMR (600 MHz, $CDCl_3$) δ (ppm) 7.51 (d, J = 8.3 Hz, 2H), 6.99 (d, J = 8.3 Hz, 2H), 3.88 (s, 3H); ^{13}C NMR (150 MHz, $CDCl_3$) δ (ppm) 158.8, 133.4, 127.8, 114.2, 55.4.

4-Nitro-1,1'-biphenyl (**6c**)

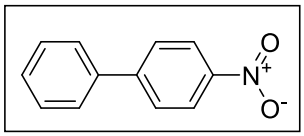

Yellow solid (88.64 mg, 89%); ^{1}H NMR (400 MHz, $CDCl_3$) δ (ppm) 8.31 (d, J = 8.8 Hz, 2H), 7.75 (d, J = 8.8 Hz, 2H), 7.65 (d, J = 6.9 Hz, 2H), 7.53 (t, J = 7.2 Hz, 2H), 7.50 – 7.45 (m, 1H); ^{13}C NMR (100 MHz, $CDCl_3$) δ (ppm) 147.6, 147.1, 138.8, 129.2, 128.9, 127.9, 127.4, 124.1.

4-Methyl-4'-nitro-1,1'-biphenyl (**6d**)

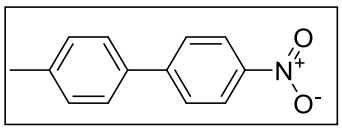

Yellow solid (95.95 mg, 90%); ^{1}H NMR (400 MHz, $CDCl_3$) δ (ppm) 8.29 (d, J = 8.9 Hz, 2H), 7.73 (d, J = 8.9 Hz, 2H), 7.55 (d, J = 8.2 Hz, 2H), 7.33 (d, J = 7.9 Hz, 2H), 2.45 (s, 3H); ^{13}C NMR (100 MHz, $CDCl_3$) δ (ppm) 147.6, 146.9, 139.1, 135.9, 129.9, 127.5, 127.2, 124.1, 21.2.

1-(4'-methoxy-[1,1'-biphenyl]-4-yl)ethan-1-one (**6e**)

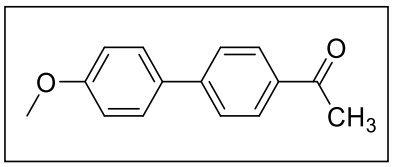

White solid (101.82 mg, 90%); ^{1}H NMR (400 MHz, $CDCl_3$) δ (ppm) 8.02 (d, J = 8.6 Hz, 2H), 7.65 (d, J = 6.6 Hz, 2H), 7.59 (d, J = 6.6 Hz, 2H), 7.01 (d, J = 9.7 Hz, 2H), 3.88 (s, 3H), 2.62 (s, 3H); ^{13}C NMR (100 MHz, $CDCl_3$) δ (ppm) 197.8, 159.9, 145.4, 135.3, 132.2, 128.9 128.4, 126.6, 55.4, 26.6.

4,4'-Dimethyl-1,1'-biphenyl (**6f**)

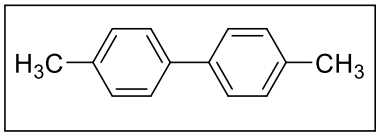

White solid (84.75 mg, 93%); ^{1}H NMR (600 MHz, $CDCl_3$) δ (ppm) 7.52 (d, J = 7.8 Hz, 2H), 7.28 (d, J = 7.8 Hz, 2H), 2.43 (s, 3H); ^{13}C NMR (150 MHz, $CDCl_3$) δ (ppm) 138.3, 136.8, 129.5, 126.8, 21.1.

1-([1,1'-Biphenyl]-4-yl)ethan-1-one (**6g**)

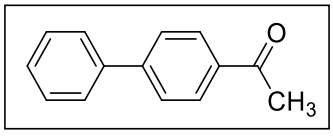

Brown solid (89.28 mg, 91%); ^{1}H NMR (400 MHz, $CDCl_3$) δ (ppm) 8.05 (d, J = 8.3 Hz, 2H), 7.70 (d, J = 8.2 Hz, 2H), 7.65 (d, J = 8.0 Hz, 2H), 7.53–7.46 (m, 2H),

7.42 (d, *J* = 7.4 Hz, 1H), 2.62 (s, 3H); ^{13}C NMR (100 MHz, $CDCl_3$) δ (ppm) 197.8, 145.8, 139.8, 128.3, 127.2, 26.7.

[1,1'-Biphenyl]-4-ol (**6h**)

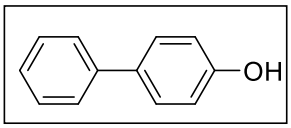

Colourless liquid (76.53 mg, 90%); ^{1}H NMR (400 MHz, $CDCl_3$) δ (ppm) 7.57 (d, *J* = 7.1 Hz, 2H), 7.51 (d, *J* = 8.7 Hz, 2H), 7.45 (t, *J* = 7.7 Hz, 2H), 7.35 (d, *J* = 7.4 Hz, 1H), 6.94 (d, *J* = 8.7 Hz, 2H); ^{13}C NMR (100 MHz, $CDCl_3$) δ (ppm) 155.1, 140.8, 134.0, 128.8, 128.4, 126.8, 115.7.

5.5.3 Representative ^{1}H and ^{13}C NMR spectra of selected compounds

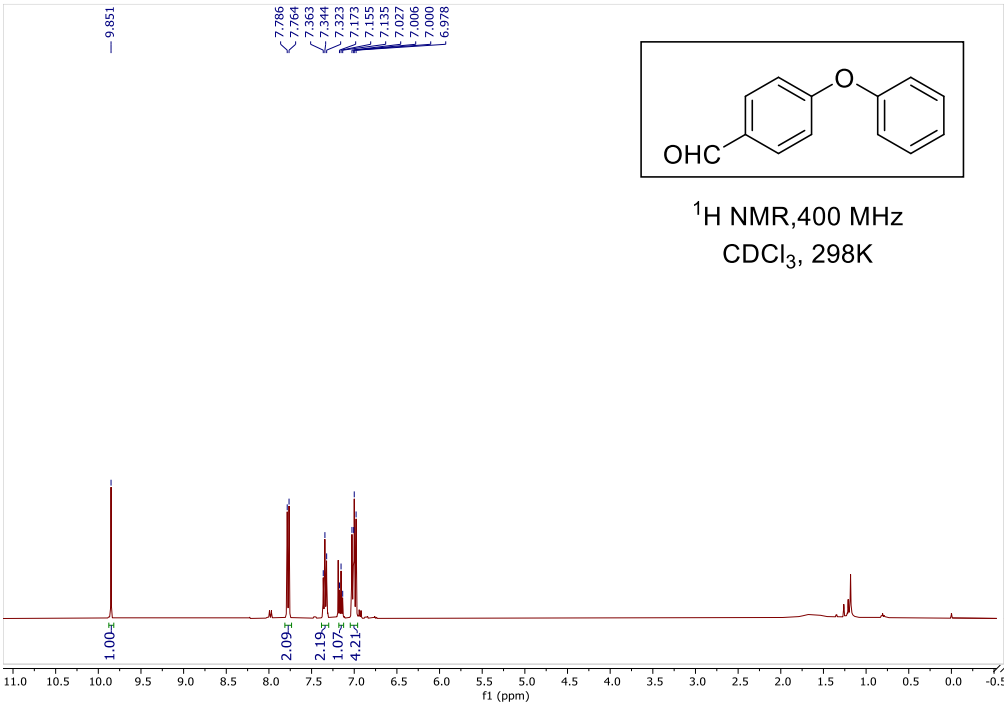

Figure **5.11** ^{1}H NMR Spectrum of **3a** in $CDCl_3$

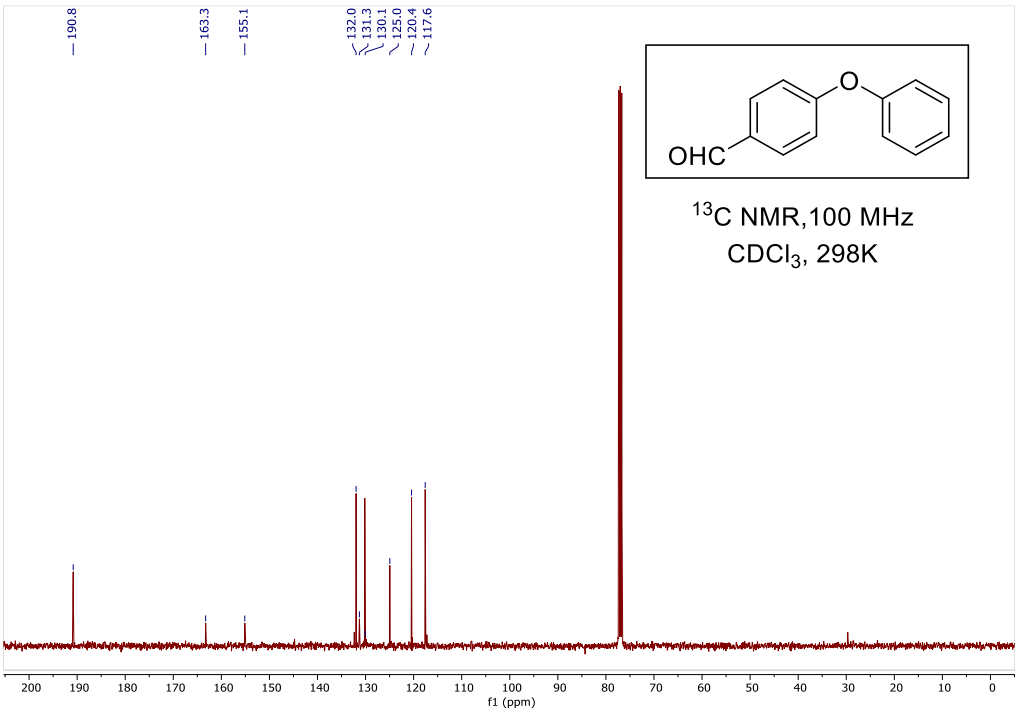

Figure **5.12** ^{13}C NMR Spectrum of **3a** in $CDCl_3$

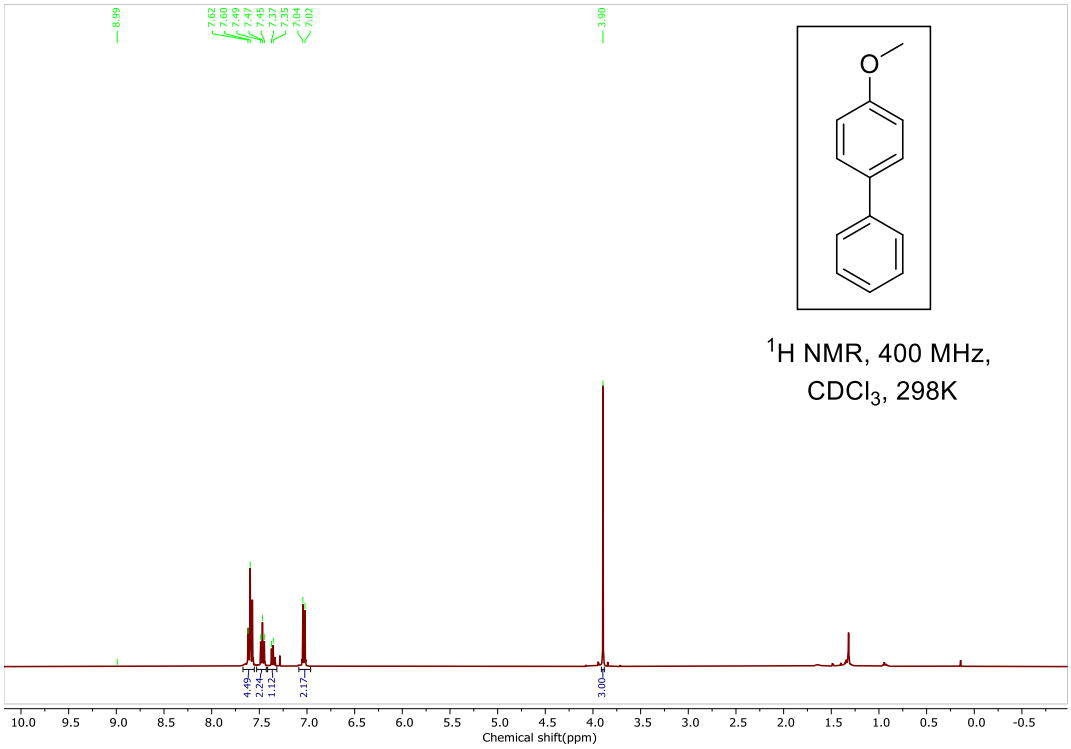

Figure **5.13** ^{1}H NMR Spectrum of **6a** in $CDCl_3$

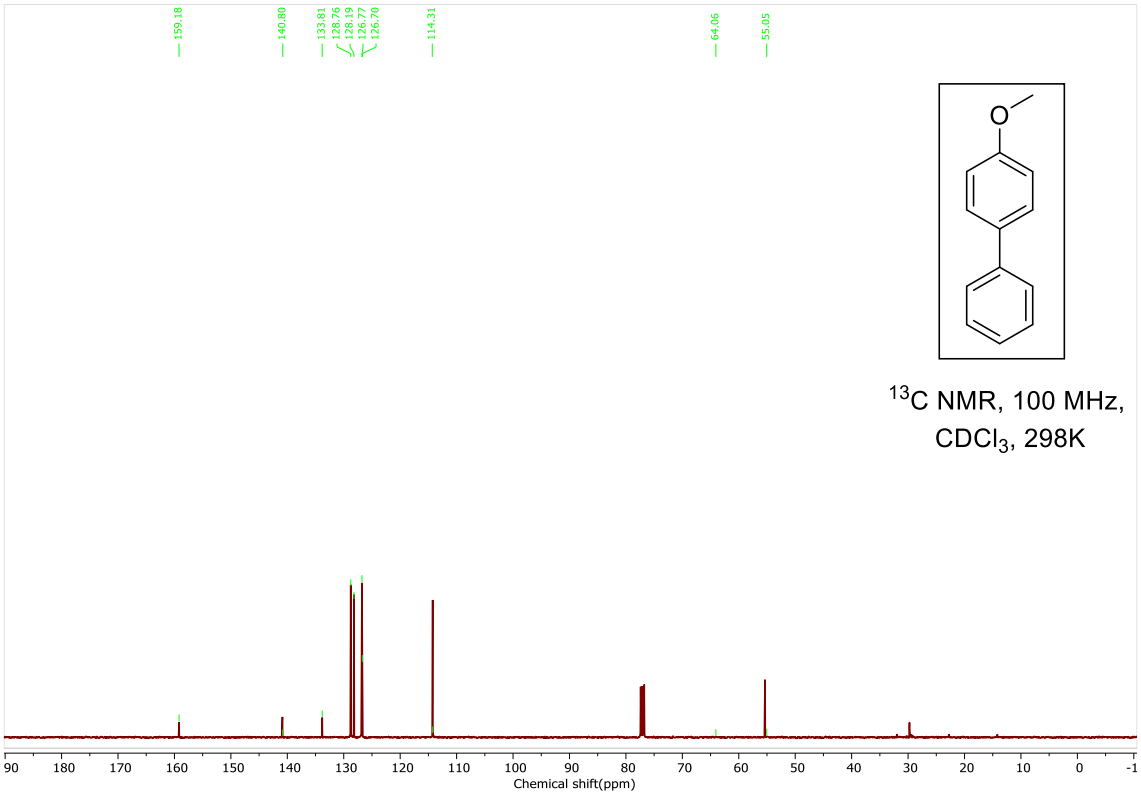

Figure **5.14** ^{13}C NMR Spectrum of **6a** in $CDCl_3$

5.6 Bibliography

[1] Ruiz-Castillo, P. and Buchwald, S. L. Applications of palladium-catalysed C–N cross-coupling reactions. *Chemical Reviews*, 116(19):12564-12649, 2016.

[2] Johansson Seechurn, C. C., Kitching, M. O., Colacot, T. J., and Snieckus, V. Palladium-catalysed cross-coupling: a historical contextual perspective to the 2010 Nobel Prize. *Angewandte Chemie International Edition*, 51(21):5062-5085, 2012.

[3] Campeau, L.-C. and Hazari, N. Cross-coupling and related reactions: connecting past success to the development of new reactions for the future. *Organometallics*, 38(1):3-35, 2018.

[4] Yasuda, N. Application of cross-coupling reactions in Merck. *Journal of Organometallic Chemistry*, 653(1-2):279-287, 2002.

[5] Biffis, A., Centomo, P., Del Zotto, A., and Zecca, M. Pd metal catalysts for cross-couplings and related reactions in the 21st century: a critical review. *Chemical Reviews*, 118(4):2249-2295, 2018.

[6] Han, F.-S. Transition-metal-catalysed Suzuki–Miyaura cross-coupling reactions: a remarkable advance from palladium to nickel catalysts. *Chemical Society Reviews*, 42(12):5270-5298, 2013.

[7] Trzeciak, A. and Augustyniak, A. The role of palladium nanoparticles in catalytic C–C cross-coupling reactions. *Coordination Chemistry Reviews*, 384:1-20, 2019.

[8] Zhu, Y., Dong, W., and Tang, W. Palladium-catalysed cross-couplings in the synthesis of agrochemicals. *Advanced Agrochem*, 2022.

[9] Devendar, P., Qu, R.-Y., Kang, W.-M., He, B., and Yang, G.-F. Palladium-catalysed cross-coupling reactions: a powerful tool for the synthesis of agrochemicals. *Journal of Agricultural and Food Chemistry*, 66(34):8914-8934, 2018.

[10] So, C. M. and Kwong, F. Y. Palladium-catalysed cross-coupling reactions of aryl mesylates. *Chemical Society Reviews*, 40(10):4963-4972, 2011.

[11] Yin, L. and Liebscher, J. Carbon− carbon coupling reactions catalysed by heterogeneous palladium catalysts. *Chemical Reviews*, 107(1):133-173, 2007.

[12] Chen, A. and Ostrom, C. Palladium-based nanomaterials: synthesis and electrochemical applications. *Chemical Reviews*, 115(21):11999-12044, 2015.

[13] Arif, M. A Critical Review of Palladium Nanoparticles Decorated in Smart Microgels. *Polymers*, 15(17):3600, 2023.

[14] Hill, N. J., Bowman, M. D., Esselman, B. J., Byron, S. D., Kreitinger, J., and Leadbeater, N. E. Ligand-free Suzuki–Miyaura coupling reactions using an inexpensive aqueous palladium source: A synthetic and computational exercise for the undergraduate organic chemistry laboratory. *Journal of Chemical Education*, 91(7):1054-1057, 2014.

[15] Vásquez-Céspedes, S., Betori, R. C., Cismesia, M. A., Kirsch, J. K., and Yang, Q. Heterogeneous catalysis for cross-coupling reactions: an underutilized powerful and sustainable tool in the fine chemical industry? *Organic Process Research & Development*, 25(4):740-753, 2021.

[16] Farhang, M., Akbarzadeh, A. R., Rabbani, M., and Ghadiri, A. M. A retrospective-prospective review of Suzuki–Miyaura reaction: From cross-coupling reaction to pharmaceutical industry applications. *Polyhedron*: 116124, 2022.

[17] Mukai, S. and Yamada, Y. Catalyst Recycling in the Suzuki Coupling Reaction: Toward a Greener Synthesis in the Pharmaceutical Industry. *Knowledge*, 3(1):1-17, 2022.

[18] Fihri, A., Bouhrara, M., Nekoueishahraki, B., Basset, J.-M., and Polshettiwar, V. Nanocatalysts for Suzuki cross-coupling reactions. *Chemical Society Reviews*, 40(10):5181-5203, 2011.

[19] Busch, M., Wodrich, M. D., and Corminboeuf, C. A generalized picture of C–C cross-coupling. *ACS Catalysis*, 7(9):5643-5653, 2017.

[20] Marčeková, M., Ferko, B., Detková, K. R., and Jakubec, P. Denitrative cross-couplings of nitrostyrenes. *Molecules*, 25(15):3390, 2020.

[21] Kashihara, M. and Nakao, Y. Cross-coupling reactions of nitroarenes. *Accounts of Chemical Research*, 54(14):2928-2935, 2021.

[22] Muto, K., Okita, T., and Yamaguchi, J. Transition-metal-catalysed denitrative coupling of nitroarenes. *ACS Catalysis*, 10(17):9856-9871, 2020.

[23] Zou, D., Wang, W., Hu, Y., and Jia, T. Nitroarenes and nitroalkenes as potential amino sources for the synthesis of N-heterocycles. *Organic & Biomolecular Chemistry*, 21(11):2254-2271, 2023.

[24] Chen, T., Xiong, H., Yang, J.-F., Zhu, X.-L., Qu, R.-Y., and Yang, G.-F. Diaryl ether: A privileged scaffold for drug and agrochemical discovery. *Journal of Agricultural and Food Chemistry*, 68(37):9839-9877, 2020.

[25] Wei, Q., Wang, Z.-P., Zhang, X., and Zou, Y. Diaryl ether formation by a versatile thioesterase domain. *Journal of the American Chemical Society*, 144(22):9554-9558, 2022.

[26] Kikelj, D. Recent progress in diaryl ether synthesis. *Synthesis*, 2006(14):2271-2285, 2006.

[27] Chen, J., Wang, X., Zheng, X., Ding, J., Liu, M., and Wu, H. Ligand-free copper-catalysed O-arylation of nitroarenes with phenols. *Tetrahedron*, 68(43):8905-8907, 2012.

[28] Wang, H., Yu, A., Cao, A., Chang, J., and Wu, Y. First palladium-catalysed denitrated coupling reaction of nitroarenes with phenols. *Applied Organometallic Chemistry*, 27(10):611-614, 2013.

[29] Begum, T., Mondal, M., Borpuzari, M. P., Kar, R., Gogoi, P. K., and Bora, U. Palladium-on-Carbon-Catalysed Coupling of Nitroarenes with Phenol: Biaryl Ether Synthesis and Evidence of an Oxidative-Addition-Promoted Mechanism. *European Journal of Organic Chemistry*, 2017(22):3244-3248, 2017.

[30] Zamiran, F. and Ghaderi, A. Nickel-catalysed denitrative etherification of activated nitrobenzenes. *Journal of the Iranian Chemical Society*, 16(2):293-299, 2019.

[31] Yadav, M. R., Nagaoka, M., Kashihara, M., Zhong, R.-L., Miyazaki, T., Sakaki, S., and Nakao, Y. The Suzuki–Miyaura coupling of nitroarenes. *Journal of the American Chemical Society*, 139(28):9423-9426, 2017.

[32] Feng, B., Yang, Y., and You, J. A methylation platform of unconventional inert aryl electrophiles: trimethylboroxine as a universal methylating reagent. *Chemical Science*, 11(23):6031-6035, 2020.

[33] Inoue, F., Kashihara, M., Yadav, M. R., and Nakao, Y. Buchwald–Hartwig amination of nitroarenes. *Angewandte Chemie International Edition*, 56(43):13307-13309, 2017.

[34] Feng, B., Yang, Y., and You, J. Palladium-catalysed denitrative Sonogashira-type cross-coupling of nitrobenzenes with terminal alkynes. *Chemical Communications*, 56(5):790-793, 2020.

[35] Okita, T., Asahara, K. K., Muto, K., and Yamaguchi, J. Palladium-catalysed Mizoroki–Heck reaction of nitroarenes and styrene derivatives. *Organic Letters*, 22(8):3205-3208, 2020.

[36] Hooshmand, S. E., Heidari, B., Sedghi, R., and Varma, R. S. Recent advances in the Suzuki–Miyaura cross-coupling reaction using efficient catalysts in eco-friendly media. *Green Chemistry*, 21(3):381-405, 2019.

[37] Mpungose, P. P., Vundla, Z. P., Maguire, G. E., and Friedrich, H. B. The current status of heterogeneous palladium catalysed Heck and Suzuki cross-coupling reactions. *Molecules*, 23(7):1676, 2018.

[38] Gao, M., Wang, J., Shang, W., Chai, Y., Dai, W., Wu, G., Guan, N., and Li, L. Zeolite-encaged palladium catalysts for heterogeneous Suzuki-Miyaura cross-coupling reactions. *Catalysis Today*, 410:237-246, 2023.

[39] Hussain, I., Capricho, J., and Yawer, M. A. Synthesis of Biaryls via Ligand-Free Suzuki–Miyaura Cross-Coupling Reactions: A Review of Homogeneous and Heterogeneous Catalytic Developments. *Advanced Synthesis & Catalysis*, 358(21):3320-3349, 2016.

[40] Das, P., Sharma, D., Shil, A. K., and Kumari, A. Solid-supported palladium nano and microparticles: an efficient heterogeneous catalyst for ligand-free Suzuki–Miyaura cross-coupling reaction. *Tetrahedron Letters*, 52(11):1176-1178, 2011.

[41] Ashraf, M., Ahmad, M. S., Inomata, Y., Ullah, N., Tahir, M. N., and Kida, T. Transition metal nanoparticles as nanocatalysts for Suzuki, Heck and Sonogashira cross-coupling reactions. *Coordination Chemistry Reviews*, 476:214928, 2023.

[42] Pagliaro, M., Pandarus, V., Ciriminna, R., Béland, F., and Demma Carà, P. Heterogeneous versus homogeneous palladium catalysts for cross-coupling reactions. *ChemCatChem*, 4(4):432-445, 2012.

[43] Van Vaerenbergh, B., Lauwaert, J., Vermeir, P., De Clercq, J., and Thybaut, J. W. Synthesis and support interaction effects on the palladium nanoparticle catalyst characteristics. *Advances in Catalysis*, 65:1-120, 2019.

[44] Shi, G. and Dong, Z. Palladium Supported on Porous Organic Polymer as Heterogeneous and Recyclable Catalyst for Cross Coupling Reaction. *Molecules*, 27(15):4777, 2022.

[45] Hoseini, S. J., Heidari, V., and Nasrabadi, H. Magnetic Pd/Fe3O4/reduced-graphene oxide nanohybrid as an efficient and recoverable catalyst for Suzuki–Miyaura coupling reaction in water. *Journal of Molecular Catalysis A: Chemical*, 396:90-95, 2015.

[46] Djakovitch, L. and Koehler, K. Heck reaction catalysed by Pd-modified zeolites. *Journal of the American Chemical Society*, 123(25):5990-5999, 2001.

[47] Alapour, S., Farahani, M. D., Ramjugernath, D., Koorbanally, N. A., and Friedrich, H. B. Ligand free heterogeneous Sonogashira cross-coupling reaction over an in situ Organoiodine capsulized palladium anchored to a perovskite catalyst. *ACS Sustainable Chemistry & Engineering*, 7(15):12697-12706, 2019.

[48] Wu, C., Peng, X., Zhong, L., Li, X., and Sun, R. Green synthesis of palladium nanoparticles via branched polymers: a bio-based nanocomposite for C–C coupling reactions. *RSC Advances*, 6(38):32202-32211, 2016.

[49] Varma, R. S. Biomass-derived renewable carbonaceous materials for sustainable chemical and environmental applications. *ACS Sustainable Chemistry & Engineering*, 7(7):6458-6470, 2019.

[50] Chao, M., Zhang, G., Li, Z., Liu, L., Yan, S., Chen, Y., Shi, Y., Yan, X., and Cao, C. Synthesis of Pd nanoparticles supported on the three-dimensional mesostructured of hardwood and its application. *ChemistrySelect*, 4(3):766-773, 2019.

[51] Rizzo, G., Albano, G., Lo Presti, M., Milella, A., Omenetto, F. G., and Farinola, G. M. Palladium Supported on Silk Fibroin for Suzuki–Miyaura Cross-Coupling Reactions. *European Journal of Organic Chemistry*, 2020(45):6992-6996, 2020.

[52] Easson, M. W., Jordan, J. H., Bland, J. M., Hinchliffe, D. J., and Condon, B. D. Application of Brown Cotton-Supported Palladium Nanoparticles in Suzuki–

Miyaura Cross-Coupling Reactions. *ACS Applied Nano Materials*, 3(7):6304-6309, 2020.

[53] Baruah, D., Das, R. N., Hazarika, S., and Konwar, D. Biogenic synthesis of cellulose supported Pd (0) nanoparticles using hearth wood extract of Artocarpus lakoocha Roxb—A green, efficient and versatile catalyst for Suzuki and Heck coupling in water under microwave heating. *Catalysis Communications*, 72:73-80, 2015.

[54] Akgül, M., Korkut, S., Çamlıbel, O., and Ayata, Ü. Some Chemical Properties of Luffa and Its Suitability for Medium Density Fiberboard (MDF) Production. *BioResources*, 8(2), 2013.

[55] Dewan, A., Sarmah, M., Bharali, P., Thakur, A. J., Boruah, P. K., Das, M. R., and Bora, U. Pd nanoparticles-loaded honeycomb-structured bio-nanocellulose as a heterogeneous catalyst for heteroaryl cross-coupling reaction. *ACS Sustainable Chemistry & Engineering*, 9(2):954-966, 2021.

[56] Tanobe, V. O., Flores-Sahagun, T. H., Amico, S. C., Muniz, G. I., and Satyanarayana, K. Sponge gourd (Luffa cylindrica) reinforced polyester composites: preparation and properties. *Defence Science Journal*, 64(3):273, 2014.

[57] Kazemi Tabrizi, A., Khademieslam, H., Hemmasi, A. H., Bazyar, B., and Atghia, S. V. Luffa as a lignocellulosic material for fabrication of a new and green catalyst in promoting of coumarin and bis(indolyl)methane derivatives. *Green Chemistry Letters and Reviews*, 13(4):328-340, 2020.

[58] Lai, S., Gao, J., Zhang, H., Cheng, L., and Xiong, X. Luffa sponge supported dendritic imidazolium ILs with high-density active sites as highly efficient and environmentally friendly catalysts for CO_2 chemical fixation. *Journal of CO_2 Utilization*, 38:148-157, 2020.

[59] Valero-Romero, M. J., Rodríguez-Cano, M. Á., Palomo, J., Rodríguez-Mirasol, J., and Cordero, T. Carbon-based materials as catalyst supports for Fischer–Tropsch synthesis: a review. *Frontiers in Materials*, 7:617432, 2021.

[60] Hospodarova, V., Singovszka, E., and Stevulova, N. Characterization of cellulosic fibers by FTIR spectroscopy for their further implementation to building materials. *American Journal of Analytical Chemistry*, 9(6):303-310, 2018.

[61] Boeriu, C. G., Bravo, D., Gosselink, R. J., and van Dam, J. E. Characterisation of structure-dependent functional properties of lignin with infrared spectroscopy. *Industrial Crops and Products*, 20(2):205-218, 2004.

[62] Sarmah, M., Neog, A. B., Boruah, P. K., Das, M. R., Bharali, P., and Bora, U. Effect of substrates on catalytic activity of biogenic palladium nanoparticles in C–C cross-coupling reactions. *ACS Omega*, 4(2):3329-3340, 2019.

[63] Guo, Z., Liu, T., Li, W., Zhang, C., Zhang, D., and Pang, Z. Carbon Supported Oxide-Rich Pd-Cu Bimetallic Electrocatalysts for Ethanol Electrooxidation in Alkaline Media Enhanced by Cu/CuO x. *Catalysts*, 6(5):62, 2016.

[64] Yaradoddi, J. S., Banapurmath, N. R., Ganachari, S. V., Soudagar, M. E. M., Sajjan, A. M., Kamat, S., Mujtaba, M., Shettar, A. S., Anqi, A. E., and Safaei, M. R. Bio-based material from fruit waste of orange peel for industrial applications. *Journal of Materials Research and Technology*, 17:3186-3197, 2022.

[65] Bhattacharjee, P., Dewan, A., Boruah, P. K., Das, M. R., Mahanta, S. P., Thakur, A. J., and Bora, U. Bimetallic Pd–Ag nanoclusters decorated micro-cellulose bio-template towards efficient catalytic Suzuki–Miyaura coupling reaction of nitrogen-rich heterocycles. *Green Chemistry*, 24(18):7208-7219, 2022.

[66] Huang, C., Shi, F., Cui, Y., Li, C., Lin, J., Liu, Q., Qin, A., Wang, H., Wu, G., and Wu, P. A palladium-catalysed approach to allenic aromatic ethers and first total synthesis of terricollene A. *Chemical Science*, 12(27):9347-9351, 2021.

[67] Yu, Y., Zhao, Y., Huang, T., and Liu, H. Shape-controlled synthesis of palladium nanocrystals by microwave irradiation. *Pure and Applied Chemistry*, 81(12):2377-2385, 2009.

[68] Braga, A. A., Morgon, N. H., Ujaque, G., and Maseras, F. Computational characterization of the role of the base in the Suzuki− Miyaura cross-coupling reaction. *Journal of the American Chemical Society*, 127(25):9298-9307, 2005.